Sleep-wake dynamics and EEG

in a rat model of Prolonged Photoperiod

Louise Haugen Bjerrum

MAPSYK360, master's program in psychology,

specialization: Behavioral Neuroscience

at

THE UNIVERSITY OF BERGEN

FACULTY OF PSYCHOLOGY

SPRING 2018

Main supervisor: Janne Grønli

Department of Biological and Medical Psychology, University of Bergen, Norway

Co-supervisor: Jelena Mrdalj

Department of Biological and Medical Psychology, University of Bergen, Norway

Co-supervisor: Michael Rempe

Department of Mathematics and Computer Science, Whitworth University, US

Abstract

Light exerts a strong influence on our physiology and behavior. It has been suggested that blue-enriched light promotes alertness in both humans and rodents through signaling via intrinsic photosensitive retinal ganglion cells (ipRGCs).

The aims of this study were 1) to validate a semi-automatic sleep scoring algorithm in rats, and 2) to use the algorithm to characterize the long-term effects of prolonged photoperiod on sleep-wake dynamics, sleep consolidation, electrophysiological changes, and homeostatic sleep regulation in rats.

Rats (n=6/group) were housed in 12:12 LD cycle for baseline, 7 days of exposure to prolonged photoperiod 20:4 LD in either white or blue-enriched light, followed by 7 days recovery in 12:12 LD. Sleep (electroencephalography and electromyography) was recorded continuously by means of telemetry.

Results from the validation of a semi-automatic sleep scoring algorithm showed that the algorithm performed with a substantial agreement compared to a gold standard manually scored.

Rats exposed to seven days of prolonged photoperiod in white light spent more time asleep (total sleep, and slow-wave sleep (SWS)), showed stronger sleep consolidation (more SWS and REM sleep bouts), and spent less time awake. In contrast, prolonged blue-enriched light exposure did not exert any changes in sleep-wake dynamics. However, a suppressing effect on beta activity in quiet wakefulness was evident during blue-enriched light exposure, an effect that lasted throughout the entire recovery period. Exposure to prolonged photoperiod exerted minor effects on the homeostatic regulation of sleep.

Overall, exposure to prolonged photoperiod induced changes in sleep and wakefulness and results point towards an alerting effect of blue-enriched light that persisted for at least one week in normal light conditions.

Sammendrag

Lys har en sterk innflytelse på vår fysiologi og atferd. Det har blitt foreslått at blå-beriket lys fremmer årvåkenhet, både hos mennesker og hos rotter via signaloverføring fra fotosensitive ganglionceller i retina («ipRGCs»).

Hensiktene med denne studien var 1) å validere en semi-automatisk søvnskåringsalgoritme hos rotter, og 2) å bruke algoritmen til å karakterisere de langvarige effektene av forlenget fotoperiode på søvn-våkenhetsdynamikker, søvnkonsolidering, elektrofysiologiske endringer og homeostatisk søvnregulering hos rotter.

Rottene (n=6/gruppe) ble oppstallet i en 12:12 lys-mørke (LD) syklus i baseline, etterfulgt av syv dager med eksponering for forlenget fotoperiode 20:4 LD i enten hvitt eller blå-beriket lys, etterfulgt av syv dager i gjenhenting i 12:12 LD. Søvn (elektroencefalografi og elektromyografi) ble målt kontinuerlig med telemetri.

Resultater fra valideringen av den semi-automatiske søvnskåringsalgoritmen viste at algoritmen utviste betydelig grad av overensstemmelse med gull-standarden manuell skåring.

Rotter som ble eksponert for syv dager forlenget fotoperiode i hvitt lys tilbragte mer tid i søvn (mer total søvn og 'slow-wave'-søvn (SWS)), viste sterkere søvnkonsolidering (flere SWS- og 'rapid eye movement'(REM)-søvnepisoder) og tilbragte mindre tid i våkenhet. Blå-beriket lyseksponering induserte ingen endringer i søvn-våkenhetsdynamikker. Dog ble det observert en undertrykkelse av beta-aktivitet under avslappet våkenhet etter blå-beriket lys, og effekten vedvarte ut gjenhentingsperioden. Eksponering til forlenget fotoperiode hadde svært få effekter på den homeostatiske reguleringen av søvn.

Oppsummert induserte forlenget fotoperiode endringer i søvn og våkenhet og resultatene peker mot en aktiverende effekt av blå-beriket lys som vedvarte i minst én uke under normale lysbetingelser.

Acknowledgements

First of all, I want to thank my main supervisor, Janne Grønli, for everything you have thought me in these three years. You have introduced me to the highly fascinating field of sleep science, and the passion and interest you share for science has been truly inspiring. I also want to thank you for giving me the opportunity to collaborate with great international sleep researchers.

Second, I want to thank my co-supervisor Jelena Mrdalj for always taking the time to explain and discuss both difficult and important things, and for always being in such a good mood. Your love for science, dance and music has been uplifting in all this time.

To my co-supervisor Michael Rempe, thank you for making it possible for me to dig a bit into the world of algorithms, and for taking the time to explain mathematical concepts in ways that a non-mathematician can understand.

To Andrea and Torhild, thank you for being there for me both as close friends and colleagues. I highly appreciate our endless number of coffee breaks, chit chats about life, and all the help you could offer in the hardest times of writing. Andrea, thank you for help with making figures, and Torhild, thank you for handling my references and for taking on the role as psychiatric nurse in times of need.

To my closest friends and family, thank you for always believing in me and supporting me no matter what. And to my dearest Kine, thank you for keeping up with the past few months and for making life a lot more enjoyable despite tough times of writing.

Last, I want to thank all fellow members of Bergen Stress and Sleep Group for creating such a positive and inspiring research environment. You have all inspired me, one way or another.

My contribution to the dataset in this thesis

In the end of spring 2016, the second semester of my master programme, I was invited to take part in the development of methods crucial for the analysis of data presented in this thesis. At the time, I was being trained by Jelena Mrdalj in manual scoring of sleep in the rat. Each of the 23 datasets was of 21 days duration, making manual sleep scoring a highly labor intensive and time consuming process. We were therefore in need of efficient sleep scoring tools, as well as software capable of processing and giving detailed analysis of sleep across the 21 days. Janne Grønli made it possible for me to collaborate with two colleagues of hers; Associate Professor Jonathan Wisor and Associate Professor Michael Rempe.

Throughout the period May-October 2016, I scored approximately 1 043 280 epochs (1 epoch = 10 s). In the months to follow I collaborated with Dr. Rempe in further developing a semi-automatic sleep scoring algorithm. I performed test-runs, engaged in trouble-shooting, and suggested adjustments in the algorithm. The final algorithm was subsequently applied to all sleep recordings. Several members of the research team offered great help in the rescoring of data.

In spring 2017 I collaborated closely with Dr. Wisor in the development and improvement of an algorithm aiming at efficient and advanced processing and analysis of polysomnographic data. Over the course of the following months I tested consecutive versions of the algorithm, provided feedback, and took an active part in Skype discussions aiming at fine-tuning the algorithm to our research interests. The final result after several months of work was the downloadable *SLEEP report* app; a computer program capable of performing detailed processing and analysis of local data files.

In the early spring 2018, Bergen Stress and Sleep Group got a renewed interest in the two-process model of sleep regulation. My interest in the model was also renewed and as a

consequence of this interest, I formulated hypotheses on the effects of light on one of the two processes in the original model. At the same time, a second collaboration with Dr. Rempe was initiated on mathematical modeling of the very same process in the two-process of sleep regulation. Dr. Rempe performed the simulations, I analyzed the output.

Table of contents

Contents

Abbreviations

ACh	acetylcholine
AW	active wakefulness
ANOVA	analysis of variance
BF	basal forebrain
BD	bipolar disorder
BB	blue-blocking
D	dark
Td	declining time constant
DA	dopamine
EEG	electroencephalography
EMG	electromyography
EOG	electrooculography
FF	fronto-frontal
FP	fronto-parietal
fMRI	functional magnetic resonance imaging
GABA	gamma-aminobutyric acid
Hz	hertz
h	hour
IGL	intergeniculate leaflet
IF	image forming
ipRGC	intrinsic photosensitive retinal ganglion cell
KO	knock-out
LH	lateral hypothalamus
LSD	least significant difference

LED	light-emitting diode
L	light
LD	light-dark
LDT	laterodorsal tegmental nucleus
LC	locus coeruleus
LA	lower asymptote
MCH	melanin-concentrating hormone
ms	milliseconds
nm	nanometer
NE	norepinephrine
NIF	non-image forming
NREM	non-rapid eye movement
OPN4	opsin 4
PZ	parafacial zone
PPT	pedunculopontine tegmental nucleus
PSG	polysomnography
PCA	principal component analysis
PC	principal component
PLR	pupillary light reflex
QW	quiet wakefulness
RCT	randomized controlled trial
REM	rapid eye movement
RHT	retinohypothalamic tract
Ti	rising time constant
s	second

SLD	sublaterodorsal nucleus
SCN	suprachiasmatic nucleus
TMN	tuberomammillary nucleus
UA	upper asymptote
vSPZ	ventral subparaventricular zone
VTA	ventral tegmental area
VLPO	ventrolateral preoptic area
YMRS	Young Mania Rating Scale
ZT	zeitgeber

The advent of artificial light has significantly altered the way humans are exposed to light. We have progressively changed our lifestyle, extending the daylight hours, and exposing ourselves repeatedly to luminance pollution. Light, the circadian clock, and sleep may closely interact to allow organisms to adapt to their environments, yet to understand how prolonged light exposure may affect our physiology and brain function.

1.1. Light and Photoreception

Light is electromagnetic radiation characterized by a wave-particle duality. As a wave, light propagates through space, and the energy imparted by the wave is absorbed by molecules and atoms; giving rise to the particle-like nature of light. The energy absorbed from a wave of light is called a photon. The energy of a photon is inversely associated with the length of the wave, and thus, light of short wavelengths inherits more energy than does light of longer wavelengths.

The wave-particle duality of light mediates one of our most important senses, namely that of vision. In the retina, a delicate neural tissue located in the back of the eye ball, we find assemblies of sensory neurons named photoreceptors. When a beam of light strikes the photoreceptors, photons are absorbed by photopigments and photon energy is converted into neural signals that can be processed by the central nervous system. Photoreceptors of the human retina are able to detect electromagnetic radiation in the range of approximately 380 to 750 nanometers (nm). The “classical” photoreceptors of the mammalian retina are the rods and cones. Rods are involved in black-and-white vision and express the photopigment rhodopsin, which is maximally sensitive to light of ~500 nm. Cones are responsible for the perception of color and display different spectral sensitivities depending on which opsin they express. Short(S)-wavelength cones express cyanolabe showing a peak sensitivity at ~420 nm,

medium(M)-wavelength cones express chlorolabe with a peak sensitivity at ~535 nm, and long(L)-wavelength cones express erythrolabe which is maximally sensitive at ~565 nm (Stockman & Sharpe, 2000). Rods and cones signal to bipolar cells which further synapse on retinal ganglion cells. From retinal ganglion cells, neural signals travel to the brain through the optic nerve.

1.1.1. Non-image forming Responses regulated by Light

Light not only mediates vision but also a range of non-image forming (NIF) responses, including the suppression of melatonin secretion from the pineal gland, constriction of pupils (the pupillary light reflex, PLR), suppression of locomotor activity in nocturnal species (negative masking), and entrainment of the circadian clock to the ambient light-dark (LD) cycle (circadian photoentrainment) (Golombek & Rosenstein, 2010). For over 150 years it was believed that rods and cones were the photoreceptors responsible for NIF responses to light. However, following a decade of research, we now know that these responses are primarily conveyed through a third class of specialized retinal photoreceptors. The discovery of these novel photoreceptors emanated from research aiming at elucidating aspects of circadian photoentrainment.

1.1.2. Circadian photoentrainment

During the evolution of life, the daily solar cycle has been one of the most predictable features of the biosphere. Together with the rotation of the earth around its own axis, the Sun has imposed rhythmic variations in the LD environment to which organisms have adapted their physiology and behavior in the temporal domain. Daily rhythms in physiology and behavior are regulated by a biological “master clock” located in the suprachiasmatic nucleus (SCN) of the hypothalamus. The intrinsic period of the SCN is slightly longer than 24h, but is entrained

to external time cues (‘zeitgebers’; meaning “time-givers”) on a day-to-day basis (Aschoff, 1965). Light is the strongest zeitgeber in the external environment, in where both the quantity and quality of light throughout the 24h serve as entrainment cues (Roenneberg & Foster, 1997). The entrainment of the circadian clock to light is facilitated through the retinohypothalamic tract (RHT) – a monosynaptic pathway from retinal photoreceptors to neurons of the SCN (Moore & Lenn, 1972).

1.1.3. The discovery of a novel photoreceptor system in the retina

In the search for the retinal photoreceptive cells mediating circadian photoentrainment through the RHT, a set of observations from both animal and human studies raised the possibility that photoreceptors other than the classical rods and cones were the ones mediating circadian responses to light. First, it was shown that mice with natural occurring retinal mutations causing complete loss of rods and ~95% loss of cones were still able to entrain their circadian rhythm to light (Provencio, Wong, Lederman, Argamaso, & Foster, 1994). From human studies, it became known that, despite suffering from blindness and visual impairments, some patients still presented with suppression of melatonin secretion in response to bright light exposure (Czeisler et al., 1995). In order to clarify whether the small set of preserved cones (~5%) in mutated mice were sufficient for maintaining circadian photoentrainment, mice were genetically modified to lack all functional rods and cones. Despite this genetic modification, mice showed normal circadian photoentrainment of wheel-running behavior (Freedman et al., 1999) and suppression of melatonin secretion (Lucas, Freedman, Muñoz, Garcia-Fernández, & Foster, 1999).

In 2002, Berson and colleagues solved a substantial portion of the puzzle when they identified a subset of retinal ganglion cells in the rat RHT that were shown to be photosensitive in the absence of inputs from rods, cones and other retinal neurons (Berson,

Dunn, & Takao, 2002). Hence, these cells were named intrinsic photosensitive retinal ganglion cells (ipRGCs), and unlike the classical photoreceptors being hyperpolarized by light, ipRGCs responded with depolarization (increased firing rate) (Berson et al., 2002). The photopigment responsible for the photosensitivity of ipRGCs was found to be melanopsin (Hannibal, 2002; Hattar, Liao, Takao, Berson, & Yau, 2002; Provencio et al., 2000). Melanopsin, originally identified in the light-sensitive melanophores of frog skin, shows a peak spectral sensitivity at ~479 nm (Bailes & Lucas, 2013; Panda et al., 2005), corresponding to the "blue" part of the electromagnetic spectrum. In the years following the discovery of ipRGCs and their associated photopigment, several subtypes of ipRGCs were identified. To date, five ipRGC subtypes have been characterized (M1-M5), and they differ in the expression levels of melanopsin, membrane properties, dendritic morphology, dendritic stratification, and axonal projections (Schmidt, Chen, & Hattar, 2011).

1.1.4. Axonal projections of intrinsic photosensitive retinal ganglion cells

ipRGCs project to a range of different brain regions involved in both NIF and image forming (IF) functions (Hattar et al., 2006). Here, projections of importance to circadian photoentrainment and sleep-wake regulation will be highlighted. In addition to the monosynaptic projection to SCN, ipRGCs also send direct projections to two other regions involved in circadian entrainment and negative masking of locomotor activity; the intergeniculate leaflet (IFL) of the thalamus and the hypothalamus ventral subparavenricular zone (vSPZ), respectively (Hattar et al., 2006). ipRGCs also project directly to sleep-active neurons in the ventrolateral preoptic area (VLPO) of the hypothalamus and to wake-promoting neurons located in the lateral hypothalamus (LH) (Gooley, Lu, Fischer, & Saper,

2003; Hattar et al., 2006). Through these projections, melanopsin-mediated signaling from ipRGCs exerts a direct influence on the effects of light on circadian rhythms and sleep.

1.2. Sleep

1.2.1. A brief history of the conceptualization of sleep

Up until the end of the 19th century, sleep was regarded a passive state; a phenomenon emerging from the process of reduced sensory inputs and diminished brain activity, and the reversal of this process was considered constituting the nature of being awake. In 1989 however, J. Allan Hobson, an American psychiatrist and researcher, noted that observations now supported a view of sleep as a dynamic behavior, in that sleep is *"(...) not simply the absence of waking, sleep is a special activity of the brain, controlled by elaborate and precise mechanisms"* (Pelayo & Dement, 2017). This "special activity of the brain" was first demonstrated by the German psychiatrist Hans Berger in 1928 (Berger, 1930). He recorded electrical activity from the brain surface of humans when they were asleep and awake, and these signals (or "brain waves") were given the name 'electroencephalograms'. Hence, the method of recording was called 'electroencephalography' (EEG). The main characteristics of the identified "brain waves" of sleep and wakefulness were described throughout the 1930's. In terms of EEG, wakefulness was characterized by waves of low-amplitude and an alpha rhythm (8-13 Hertz (Hz)), whereas sleep was characterized by slow waves of high-amplitude and sleep spindles (Pelayo & Dement, 2017).

Following Berger's first EEG recording and along with methodological advances in the field of sleep research and sleep medicine, researchers began elucidating the nature and workings of the neural systems regulating sleep and wakefulness. It is now acknowledged that the generation and regulation of sleep and wake states is a product of complex interactions

between several neural systems utilizing a cocktail of neurotransmitters- and peptides in the exchange of information.

1.2.2. Neural systems regulating sleep and wakefulness

A comprehensive and absolute overview of the neural mechanisms regulating sleep and wakefulness states is beyond the scope of this thesis. Therefore, a simplified description of the main regulatory systems will be presented below, emphasizing systems of importance to the discussion of findings in this thesis.

Wakefulness is regulated by two pathways ascending through the midbrain. The dorsal pathway innervates the thalamus, whereas the ventral pathway innervates the basal forebrain (BF), hypothalamus and cortex (Scammell, Arrigoni, & Lipton, 2017). These pathways promote wakefulness through the locus coeruleus (LC) producing norepinephrine (NE), the dorsal raphe and median raphe nuclei producing serotonin, the ventral tegmental area (VTA) producing dopamine (DA), and the tuberomammillary nucleus (TMN) producing histamine. In the BF and pedunculopontine tegmental nucleus (PPT), wakefulness is promoted through the signaling of acetylcholine (ACh), gamma-aminobutyric acid (GABA) and glutamate. Lastly, the lateral hypothalamus (LH) regulates wakefulness through the neuropeptides hypocretin (also called orexin) and dynorphin, as well as through glutamate and GABA.

Non-rapid eye movement (NREM) sleep is facilitated by an inhibition of wake-promoting pathways through the action of "somnogens" accumulated in the brain during wakefulness (e.g. adenosine) and an activation of sleep promoting neural regions. The neural circuits responsible for this interaction of inhibition and activation include GABAergic and galaninergic neurons in the VLPO, GABAergic neurons of the BF, and GABAergic/glycinergic neurons of the brain stem parafacial zone (PZ) (Scammell et al., 2017).

Rapid eye movement (REM) sleep is regulated by neural circuits in the pons. The central elements of these circuits are the sublaterodorsal nucleus (SLD), the PPT and the laterodorsal tegmental nucleus (LDT). In the SLD, glutamatergic neurons are responsible for generating muscle atonia characteristic of REM sleep. In PPT and LDT, neurons signaling with ACh, glutamate and GABA are involved in the regulation of REM sleep. REM sleep is also to some extent regulated by GABAergic and galaninergic neurons in the part of VLPO often referred to as "the extended VLPO" and by melanin-concentrating hormone (MCH) neurons in the lateral and posterior hypothalamus (Scammell et al., 2017).

A description of neural systems and associated neurotransmitters- and peptides is inadequate when aiming to explain the complex phenomenon of sleep regulation. Moving the description of sleep regulation up "one level" in the hierarchy, we find that the workings of neural sleep-wake regulatory systems and their associated neurotransmitters- and peptides are themselves regulated by "higher-level" factors, such as behavior, waking time, and the intensity of wakefulness. Two such "higher-level" factors constitutes the main components of what today still remains as the working model of how sleep is regulated, namely The two-process model of sleep regulation postulated by Alexander Borbély in 1982.

1.2.3. The Two-process Model of Sleep Regulation

Based on experimental studies in rats and humans, the two-process model of sleep regulation postulates that sleep is regulated by the interaction of two factors/processes: a circadian factor (process C) and a homeostatic factor (process S) (Borbély, 1982). Process C is the circadian rhythm, controlled by the "master clock", SCN, through photoentrainment by ipRGCs sending axonal projections in the RHT (see 'Non-image forming Responses regulated by Light'). Process S represents a sleep drive that rises progressively during time in wakefulness and dissipates exponentially during sleep. This sleep drive reflects the need for sleep, and its

dissipation is fundamental in order to maintain sleep homeostasis. Sleep homeostasis can be defined as *"the disposition to maintain a constant mean level of sleep by the activation of compensatory responses to sleep loss or excessive sleep"* (Franken, Tobler, & Borbély, 1995). The amount of EEG slow-wave activity (SWA; 0.5-4 Hz) in slow-wave sleep (SWS) is considered the neurophysiological marker of process S. From the analysis of human EEG recordings across 32 nights, Borbély and colleagues (Borbély, Baumann, Brandeis, Strauch, & Lehmann, 1981) determined that the initial level of SWA at sleep onset is a function of prior wake time. Not only SWA but also EEG theta activity (5-8 Hz) has been identified as a neurophysiological marker of sleep drive in the course of wakefulness (Vyazovskiy & Tobler, 2005). Recently, Grønli and colleagues examined the higher EEG frequencies and observed that EEG beta activity represents two distinct processes in two sub states of wakefulness; active wakefulness (AW, associated with active exploration and alertness) and quiet wakefulness (QW, absence of locomotion). In AW, beta EEG reflects sensory processing whereas in QW, beta EEG parallels SWA and theta activity and hence can be considered a neurophysiological marker of sleep drive (Grønli, Janne, Rempe, Clegern, Schmidt, & Wisor, 2016).

The mere time spent awake prior to sleep is not the only determinant of process S – also the "intensity" of prior wake time is of importance. In humans it has been shown that unilateral use and immobilization of one body part is associated with an increase and a decrease, respectively, in SWA over the contralateral hemispheric region (Huber et al. ,2006; Kattler et al., 1994). Similarly; rats using one paw more than the other during their active phase also show increases in SWA in the contralateral hemisphere during sleep in inactive phase (Vyazovskiy & Tobler, 2008). Thus, sleep homeostasis is not only characterized by a global component but also a local use-dependent component.

The propensity and duration of sleep is a result of the combined influences of process C and process S, illustrated in Figure 1. In a normal sleep-wake cycle, sleep drive increases throughout the waking period (W1), and sleep is initiated on a falling circadian curve (T1). The time of awakening occurs when the declining curve of process S crosses the rising curve of process C. If the waking period is extended (W2) such that sleep is initiated on a rising circadian curve (T2), the duration of the main sleep period (S2) will consequently be shorter compared to the sleep duration following sleep initiation on a falling circadian curve (S1) (Grønli, J & Ursin, 2009).

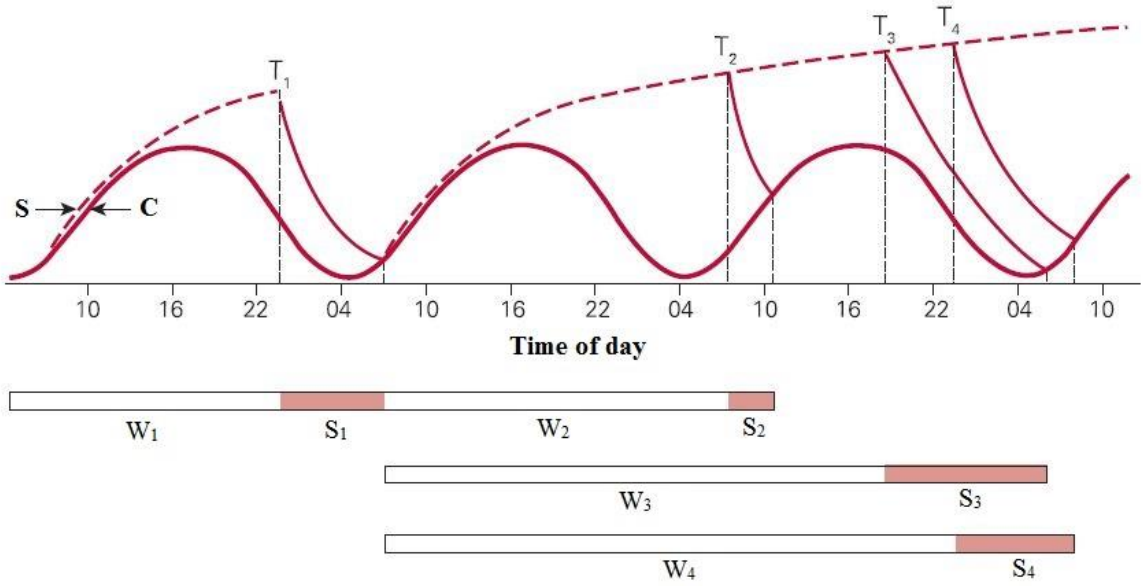

Figure 1. The duration of sleep is dependent upon an interaction between a circadian factor (C, red curve) and a homeostatic factor (S, dotted red curve). White bars (W1-W4) indicate wake periods, and red bars (S1-S4) indicate sleep periods. T1-T4 denotes the time point of initiated sleep. S rises during wake periods and dissipates during sleep periods. Awakening from the main sleep period is facilitated when the curve of S crosses the curve of C. Modified with permission from Grønli & Ursin (2009).

1.2.4. Sleep regulation in a nocturnal rodent.

Rats are nocturnal animals, with activity and wakefulness predominating in the dark phase and inactivity and sleep predominating in the light phase. Despite being nocturnal, rats display

similar features of sleep regulation to that of humans. The initial version of the two-process model of sleep regulation was in fact established to account for the regulation of sleep in rats, and was later applied to human sleep. In a series of laboratory studies performed in the 1970's- and 80's it was demonstrated that sleep in the rat is homeostatically regulated and that this regulation represents a process distinct from the circadian regulation of sleep. In 1979, Borbély and Neuhaus showed that the level of SWA rises during the animal's active (dark) phase and declines gradually in the course of SWS during the inactive (light) phase (Borbely & Neuhaus, 1979). It was also demonstrated that total sleep deprivation of 24h duration was followed by an increase in SWA during recovery SWS (Borbély, Tobler, & Hanagasioglu, 1984). Results from these two studies supported the notion of sleep being regulated by a homeostatic mechanism. Further, observations indicated that this mechanism was regulated independently of the circadian rhythm, in that a) rats with lesions of the SCN (resulting in disruption of circadian rhythmicity) still showed an increase in SWA following 24h sleep deprivation, and b) this 24h sleep deprivation did not have an effect on the phase nor period of the rest-activity rhythm in "free-running" conditions (Tobler, Borbely, & Groos, 1983) ("free-running" meaning conditions free of zeitgebers to entrain the SCN).

1.3. Effects of Light on Wakefulness and Sleep

Before the nature of the ipRGC system was characterized in terms of projections and modulating functions, it was thought that light influences wakefulness and sleep only secondary through effects on circadian photoentrainment. We now know, however, that light – via ipRGC signaling – exerts direct effects on wakefulness and sleep, both in humans and in rodents. ipRGC-mediated effects on wakefulness and sleep are a product of integrated signals from the melanopsin-driven intrinsic light response of ipRGCs and incoming signals from rods and cones transmitting their information to ipRGCs through bipolar cells. As noted

previously, each of the three photoreceptive systems of the mammalian retina present with different spectral sensitivities, meaning that the overall physiological and/or behavioral output is in large part determined by the spectral composition of the ambient light environment. In the sections to follow, effects of light on wakefulness will encompass effects on the arousal system in general; including but not limited to wakefulness, alertness, and activation.

1.3.1. Effects of light on human physiology and behavior

Studies in humans have established a prominent alerting effect of light, both during the biological day and night. During the day, exposure to polychromatic ("broadband") white light has been found to induce an acute suppression of melatonin secretion and a decrease in subjective sleepiness (Chang, A. M. et al., 2012), and decreases in alpha and alpha-theta power in the EEG (indicating reduced physiological sleepiness) (Sahin, Wood, Plitnick, & Figueiro, 2014). Exposure to monochromatic blue (460 nm) light during the biological day has also, not surprisingly considering the spectral sensitivity of melanopsin, been found to improve EEG correlates of alertness, reduce attentional lapses, and improve reaction times (Rahman et al., 2014).

The neural correlates of the alerting effects of both polychromatic and monochromatic light have been examined by the use of functional magnetic resonance imaging (fMRI). Polychromatic white light was found to be associated with activation of the posterior thalamus, in where the activation was linearly correlated with improvements in subjective alertness and increases in light intensity triggered a larger and longer-lasting response (Vandewalle et al., 2006). By comparing short-duration (50 ms) exposure to monochromatic light of different wavelengths (violet 430 nm, blue 473 nm, green 527 nm), Vandewalle and colleagues (2007) demonstrated that blue (compared to green and violet) light increased

activation in both subcortical and cortical structures, including the LC of the brain stem, the thalamus, amygdala, hippocampus, and middle frontal gyrus (Vandewalle et al., 2007).

The last decade we have experienced a boom in new light-emitting technologies such as smartphones and tablets. Several studies have also assessed the potential alerting effects of blue-enriched white light in the evening and on subsequent sleep, by comparing the effects of reading from a blue light-emitting diode (LED) device (such as tablets and smart phones) with reading from a printed book (Chang, A.-M., Aeschbach, Duffy, & Czeisler, 2015; Chellappa et al., 2013; Grønli, Janne, Byrkjedal, et al., 2016; Rångtell et al., 2016). The study performed by Chang and colleagues (2015) found that reading from an iPad was associated with reduced evening sleepiness and melatonin secretion, longer sleep latency, phase-delay of the circadian clock, and reduced alertness in the morning following light exposure. Grønli and colleagues (2016) also found that reading from an iPad for 30 minutes in bed prior to sleep decreased subjective sleepiness, and additionally, even though iPad-reading did not affect sleep time or self-reported sleep onset latency, reading from an iPad delayed the EEG dynamics of SWA by approximately 30 minutes and reduced SWA after sleep onset. Although not including an iPad/tablet reading condition, Chellappa and colleagues (2013) support the findings of Grønli, by demonstrating that a 2h exposure to blue-enriched light in the evening prior to bedtime was associated with reduced SWA in NREM sleep during the first sleep cycle. However, Rångtell and colleagues (2016) did not find any differences in sleep parameters and melatonin levels when comparing tablet reading to reading from a printed book. It should be noted that participants in this study were exposed to constant bright light for 6.5h prior to the experimental reading condition, and hence, this study is not directly comparable to that of Chang, Grønli, and Chellappa.

Monochromatic light also exerts alerting effects during the biological night when participants are kept awake. Compared to monochromatic green light, monochromatic blue

light has been shown to improve reaction times, reduce attentional lapses, increase EEG correlates of alertness, and decrease subjective sleepiness (Lockley et al., 2006; Rahman et al., 2014).

1.3.2. The effects of blocking blue light

The alerting effects of blue-enriched light can be reduced by the use of orange-tinted glasses. These glasses block out the blue wavelength range of the spectrum (hence the term blue-blocking (BB) glasses) (Gringras, Middleton, Skene, & Revell, 2015) to which the ipRGC system is the most sensitive. The use of BB glasses has been found to attenuate light-induced melatonin suppression (Kayumov et al., 2005; Sasseville, Paquet, Sévigny, & Hébert, 2006; van der Lely et al., 2015) and decrease vigilant attention and subjective alertness prior to bedtime (van der Lely et al., 2015). However, in the study by van der Lely and colleagues (2015) in where male adolescents were given BB glasses while sitting in front of LED screens, sleep the subsequent night and behavioral measures the following morning were unaffected by BB glasses, as compared to the use of clear lensed glasses as control.

BB glasses have also been used as an add-on treatment for hospitalized patients with bipolar disorder (BD) in a manic state (Henriksen et al., 2016). BD is a psychiatric illness characterized by the presence of manic and depressive episodes. Manic episodes often last several weeks, and the symptoms of such episodes include increased energy, sleep disturbances, elevated mood, irritability, risk-taking behavior, and disturbances in perception and thought. There are some indications that bipolar episodes can be triggered by changes in ambient light conditions (Bauer et al., 2015; Bauer et al., 2012). The study by Henriksen and colleagues (2016) was a randomized controlled trial (RCT) in where bipolar patients in manic state were given either BB glasses or clear-lensed glasses (placebo) to wear from 6 p.m. to 8.am for 7 consecutive days. After only 3 days of wearing BB glasses, patients presented with

a reduction in manic symptoms measured by Young Mania Rating Scale (YMRS) and the activity levels were consistently lower, compared to the control group.

1.3.3. Effect of light in rodents

In nocturnal rodents, light suppresses locomotor activity (negative masking) and promotes sleep through the signaling of ipRGCs. The importance of ipRGCs in mediating these responses comes from studies in mice genetically modified to lack the gene coding for melanopsin (Opsin 4, OPN4); referred to as OPN4-knock-out (KO) mice. Compared to wild type mice, OPN4-KO mice showed impaired sleep induction in response to white light exposure during the dark phase (Lupi, Oster, Thompson, & Foster, 2008; Muindi, Zeitzer, Colas, & Heller, 2013; Tsai et al., 2009) and an attenuated light-induced activation of the VLPO . Moreover, OPN4-KO mice slept less during a 12h L phase (due to an increased length of wake bouts), and despite a reduction in sleep time, these mice also displayed reduced SWA during most of the dark phase and during recovery sleep following a 6h sleep deprivation, indicating a prominent role of melanopsin in the regulation of sleep homeostasis (Tsai et al., 2009).

Light-induced sleep induction is indeed mediated through the ipRGC system and the effect is true for most wavelengths; however, recent observations indicate that monochromatic blue light exerts an alerting effect also in nocturnal species. By comparing the effects of monochromatic violet (405 nm), green (530 nm) and blue light (470 nm) on sleep induction, light-induced gene expression and plasma corticosterone levels in wild type and OPN4-KO mice, Pilorz and colleagues (2016) first demonstrated that, in wild type mice, green light produced a rapid sleep induction whereas blue light delayed sleep induction. In OPN4-KO mice, sleep induction was delayed in green and advanced in blue light. However, it should be noted that melanopsin is not solely responsible for light-induced sleep induction when light is administered in the dark phase; rod and cone signaling converging on ipRGCs are required for

this response (Altimus et al., 2008). Pilorz and colleagues further went on to show that, in wild type mice, blue light evoked larger increases in light-induced gene expression in the SCN and adrenal glands, whereas green light evoked larger light-induced gene expression in the VLPO. Again, blue light-induced gene expression in the SCN and adrenal glands were attenuated in OPN4-KO mice. Furthermore, compared to violet and green light, blue light induced larger increases in plasma corticosterone levels, an effect which was attenuated in OPN4-KO mice.

In summary, studies indicate that polychromatic white light promotes alertness in humans and sleep in rodents (particularly wavelengths corresponding to the "green" part of the electromagnetic spectrum), whereas blue(-enriched) light exerts an alerting effect in both species.

1.3.4. Light Exposure in the 21st Century

Daily rhythms in physiology and behavior, including the sleep-wake cycle, evolved under natural LD conditions. Under such natural conditions, the biological night begins near sunset and ends near sunrise. In the 1930s, the ambient light environment was altered dramatically when electricity was provided to power electrical light, giving humans the ability to extend the hours of light exposure during the 24h (hereafter referred to as the 'photoperiod'; the hours of light within the 24h) and to work indoors for an extended period of time. The first artificial light source was the incandescent light bulb, followed by halogen light bulbs and fluorescent lamps in the 20th century. In 2014, the Nobel Prize in Physics was awarded for the invention of the blue light-emitting diode (LED). Compared to standard light bulbs, LEDs have longer lifetimes, generate less heat and has greater efficiency. More importantly, however, is the fact that they transmit a much higher amount of blue light to the eye, compared to standard light bulbs (Tsao, Coltrin, Crawford, & Simmons, 2010). Today, the display of most televisions, computer screens, tablets and smartphones contain LEDs. Thus,

the use of LED devices beyond the normal outdoor light hours, such as during the evening and night, will signal "daytime" to the SCN and to the brain regions from which the SCN projects to. By signaling "daytime" to the master clock, exposure to blue-enriched light from LED devices at inappropriate times of day can lead to an extension of the photoperiod beyond natural conditions – an extension which may exert a profound disruption of the sleep-wake cycle. Such a disruption has been quantified in a study performed by Wright and colleague (Wright Jr et al., 2013). In this study, the effects of an electrical-lighting constructed environment were compared to the effects of a natural light environment in outdoor camping conditions in the Rocky Mountains of Colorado; that is, a light condition characterized by exposure to sun light and camp fires only. Compared to outdoor camping light conditions – in where the sun light shows a "peak" in the blue part of the spectrum around midday, the electrical-lighting constructed environment was associated with reduced exposure to sunlight during the day and increased exposure to light after sunset, and a delayed timing of the biological clock. After exposure to 1 week of outdoor camping in the Rocky Mountains, the timing of the biological clock was advances and aligned with the natural LD cycle.

1.4. A Rat Model of Prolonged Photoperiod 20:4 LD

Some of the effects on sleep and wakefulness from white and blue-enriched light exposure have been quantified in previous studies (see 'Effects of Light on Wakefulness and Sleep'). However, most of these effects are acute and/or of short-term nature. The long-term effects on sleep, wakefulness and associated changes in brain activity resulting from exposure to extended hours of light within the 24 hours largely remain uncharacterized. Using a rat model of prolonged photoperiod (20h light, 4h dark; 20:4 LD) we wanted to characterize these long-term effects. Additionally, we wanted to a) characterize the differential effects of exposure to prolonged polychromatic white light vs. blue-enriched light in order to quantify the potential

alerting effect of blue (as compared to white) light on the sleep-wake systems, and b) examine the abrupt changes resulting from a transition to 20:4 LD and back to a regular 12:12 LD cycle.

In the rat model of prolonged photoperiod, the theoretical framework and associated hypotheses were based on the two-process model of sleep regulation. Herein I have made predictions about the effects of prolonged light exposure on process S. By prolonging the hours of light within the 24h – without changing the time of lights on (ZT0), we have extended the "window" of sleep in a nocturnal rodent. The effects of prolonged photoperiod on process C, the circadian rhythm, are being characterized by other members of the research term. Due to the complexity in discussing findings I will limit the focus to process S but will hypothesize on the possible influences on process S from photoperiod-induced alterations in the "master clock" regulating process C.

1.5. Measuring Sleep

Sleep can be defined as a *"reversible behavioral state of perceptual disengagement from and unresponsiveness to the environment"*. The characteristic of reversibility distinguishes sleep from coma, and unresponsiveness to the environment – characterized by increased arousal threshold to external stimuli – distinguishes sleep from the state of quiet wakefulness. From this simple behavioral definition, sleep can be monitored in terms of changes in activity and inactivity.

Physiologically, sleep is defined in terms of changes in electrical activity of the brain, measured by EEG. In humans, changes in electrical brain activity can be detected by placing electrodes on the scalp surface. In animals, or when humans undergo surgery, EEG electrodes can be intracranial or subdural. What is really detected by EEG electrodes is the sum of excitatory postsynaptic potentials (EPSPs) generated from large neuronal assemblies with

synchronized firing (Reis, Hebenstreit, Gabsteiger, von Tscharner, & Lochmann, 2014). The generation of EPSPs occurs on a scale of milliseconds (ms), and thus EEG has high temporal resolution but low spatial resolution. When EPSPs reach the scalp surface, electrodes measure the voltage difference between EPSPs and a reference surface electrode. This voltage difference is transmitted to an impedance amplifier, and the amplified signal is sampled analog-to-digital. After filtering out noise and the like, the "clean" signal appears as rhythmic brain waves defined by their frequency (Hz); the number of cycles occurring at each second. The frequency bands most characteristic of sleep and wakefulness are: delta (0.5-4 Hz), theta (4-8 Hz), alpha (8-13 Hz), and beta (13-30 Hz).

EEG, together with the monitoring of muscle activity (electromyography, EMG) and eye movements (electrooculography, EOG) constitutes the "gold standard" of measuring sleep, namely polysomnography (PSG). On the basis of PSG, sleep stages are characterized in terms of dominating frequency bands in the background EEG, and the occurrence of transient waveform events "standing out" from the background EEG (Keenan & Hirshkowitz, 2017).

1.5.1. Sleep stages in humans

The first standardized manual for the characterization (scoring) of normal human sleep was published by Allan Rechtschaffen and Anthony Kales in 1968. In 2007, the American Academy of Sleep Medicine (AASM) published a new manual, in where events occurring during sleep and outside of "normal" brain activity were included. In addition, the new manual encompassed criteria for scoring sleep in children.

According to the AASM, human EEG is characterized by four stages: wakefulness, non-rapid eye movement sleep (NREM) 1 (N1), NREM 2 (N2), NREM 3 (N3), and rapid eye movement (REM) sleep. Wakefulness is characterized by >50% alpha activity in the occipital region and/or a) eye blinks, b) rapid eye movements and normal/high muscle tone, and c)

'reading eye' movements. N1 is a stage of drowsiness characterized by low-amplitude mixed-frequency (LAMF) or theta activity, vertex waves (sharply contoured "negative" waves; deflecting upwards), and slow eye movements. Stage N2 is characterized by the occurrence of sleep spindles ("bursts" of 12-14 Hz activity lasting ≥0.5 s) and/or K-complexes (a sharp "negative" waveform immediately followed by a large "positive" wave, lasting ≥0.5 s). Sleep spindles are generated when sensory inputs to the thalamus are reduced below a certain threshold and thalamocortical relé cells are hyperpolarized (inhibited) (McGinty & Szymusiak, 2017). N3 is the deepest stage of sleep, characterized by the presence of ≥20% slow-wave activity (SWA, 0.5-4 Hz). SWA is a product of further reduced sensory inputs to the thalamus and stronger hyperpolarization of relé cells (McGinty & Szymusiak, 2017). REM sleep is characterized by the presence of LAMF (theta- and alpha activity) without sleep spindles and K-complexes, and low muscle tone (muscle atonia, with short phasic twitches) in occurrence with phasic rapid eye movements.

1.5.2. Distribution of sleep stages in humans

Throughout a normal night's sleep, an adult enters sleep through NREM sleep, and alternates between NREM and REM sleep in cycles with durations of approximately 90-110 minutes. In the first half of the night, SWS dominates in NREM sleep episodes, reflecting the homeostatic aspect of sleep regulation (see 'The Two-process Model of Sleep Regulation'). In contrast, REM sleep is distributed towards the last part of the night and the episodes usually increase in duration as the night proceeds. See Figure 2 for an example of sleep stage distribution (called 'hypnogram') during a normal night's sleep. Across all stages of sleep, NREM sleep constitutes approximately 75-80%, whereas REM sleep constitutes approximately 20-25%. Brief awakenings are normal during the night, however these account for only about 5%.

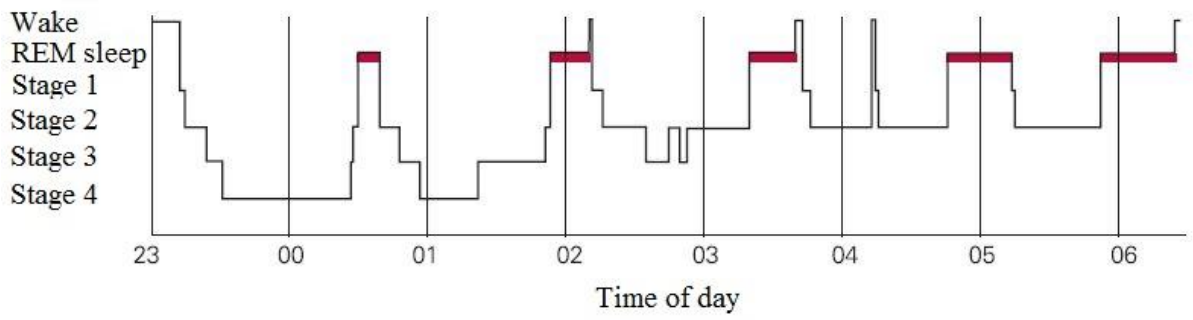

Figure 2. Hypnogram of human sleep displaying the distribution of wakefulness and sleep stages during a night-time sleep in a healthy adult free of sleep complaints. The stages of wakefulness, REM sleep and NREM sleep (S1-S4) are plotted with respect to occurrence and duration. The nomenclature of NREM sleep stages (S1-S4) are defined according to Rechtschaffen & Kales. In the AASM manual, S3 and S4 are combined to form N3. Modified from Grønli & Ursin (2009).

1.5.3. Sleep stages in rats

In rats as in humans, sleep can be characterized on the basis of dominating frequency bands in the EEG and transient waveform events. However, the number of distinct NREM sleep stages scored is reduced to either one or two stages of slow-wave sleep (SWS; SWS1 and SWS2), depending on the practices of the research laboratory. In Bergen Stress and Sleep Group (BSSG) at the University of Bergen, the following three stages are scored: wakefulness, SWS, and REM sleep. These stages are scored in epochs of 10 s duration. Roughly defined, wakefulness is characterized by low-amplitude mixed/high frequencies and moderate/high muscle tone, SWS is characterized by a predomination of delta activity, and REM sleep is characterized by a predomination of rhythmical theta activity and reduced (compared to SWS) or abolished muscle tone.

1.5.4. Distribution of sleep stages in rats

Along with being nocturnal animals (see 'Sleep regulation in a nocturnal rodent'), rats also display a polyphasic sleep pattern, meaning that even though the main sleep period is positioned to the light phase, some sleep will also occur during the dark phase. See Figure 3 for an example of a 24h hypnogram in the rat.

Figure 3. Hypnogram of rodent sleep displaying the distribution of sleep states and wakefulness across a period of 24h. White and black horizontal bar indicates 12h light phase and 12h dark phase, respectively. X=artefacts or missing signals, W=wakefulness, R=REM sleep, and S=SWS.

1.5.5. Semi-automated approaches to sleep scoring in the rat

In recent years, a handful of research laboratories have published papers describing the use of more or less "automated" methods to classify sleep and wake states in rodents (preferably mice and rats). These approaches involve the use of classification algorithms mainly rooted in the field of machine learning. Most of these algorithms rely on information inherent in the power spectra of EEG and EMG (Bastianini et al., 2014; Gilmour et al., 2010; Libourel et al., 2015; Rytkonen et al., 2011). The algorithm developed by Bastianini and colleagues (2014) was validated in several different strains of mice and rats, and across research laboratories. This algorithm displayed an overall accuracy, specificity and sensitivity of 97%, 95% and 94%, respectively. Gilmour and colleagues (2010) developed an algorithm taking advantage of the method of principal component analysis. This algorithm was validated against a set of manual (human) scorings, of which the overall agreement ranged from 93.7-94.9% and the

global kappa coefficient ranged from 0.89 to 0.91. Libourel and colleagues (2015) developed an unsupervised algorithm based on Bayesian probability classifications. The global kappa coefficient was approximately 0.7, and the specificity in classifying REM sleep reached 0.92. Lastly, the algorithm developed by Rytkonen and colleagues (2011), also using a Bayesian classifier, showed an overall agreement of 93% with manual scoring, 94-96% agreement for SWS, and 89-97% for REM sleep.

The development and improvement of classification algorithms such as those described above, is motivated by three main factors: 1) the time and resource consuming nature of scoring rodent sleep, especially in data sets of long duration, 2) the potential source of human error, and closely related to 2); 3) the lack of a standardized scoring manual. The combined action of 2) and 3) have a considerable potential of increasing both inter- and intra-rater variability among human scorers.

Sleep (EEG/EMG) recordings of which data is included in this thesis are of considerable long duration; 21 days. In the initial process of sleep scoring prior to data analysis there was a clear need of being able to ease the time and resources associated with having to classify sleep-wake states across 24h x 21 days in a total of 23 rats. A collaboration with Dr. Rempe at Whitworth University, Spokane, US, was therefore initiated. We wanted to further develop a semi-automatic sleep scoring algorithm, partly due to previous experience with the algorithm having difficulties distinguishing between wakefulness and REM sleep. The semi-automatic sleep scoring algorithm is in large part based on the algorithm described in Rempe, Clegern, & Wisor (2015). In the aforementioned publication, the algorithm was validated against manual scorings in two strains of mice (C57BL/6J (B6) and BALB/CJ (BA)). The overall percentage agreement between manual and algorithm scoring was 89%, and the global kappa value approached 0.8. For wakefulness, SWS and REMS, the agreement was 89.5%, 95.6% and 70.5%, respectively, and it was observed that, of epochs scored as

either wakefulness or REMS by a human scorer, the algorithm was more likely to score these epochs as SWS.

The specific semi-automatic algorithm used in scoring of sleep data included in this thesis has not yet been validated in rats. A validation will be undertaken in this thesis, both globally in a data set of N=20 rats, and specifically in four groups of rats exposed to different photoperiodic manipulations.

1.6. Aims and hypotheses

The first aim of this thesis is to validate a semi-automatic sleep scoring algorithm in rats. The second aim is to characterize the long-term effects of prolonged photoperiod on sleep-wake dynamics, electroencephalographic changes, and the homeostatic regulation of sleep in rats. Specifically, I aim to answer the following questions:

1) Compared to human sleep scoring, how well does a semi-automatic sleep scoring algorithm perform in the classification of sleep-wake states?
2) Are dynamics in sleep and wakefulness affected by seven days of prolonged photoperiod?
3) If sleep-wake dynamics are affected by seven days of prolonged photoperiod; are the effects attributable to changes in the homeostatic regulation of sleep?

Part I: Validation of a Semi-automatic Sleep Scoring Algorithm compared to a Gold Standard

The semi-automatic sleep scoring algorithm is hypothesized to be in at least 80% agreement with manual scoring. Due to the sensitivity of sleep stages to light, I expect that the algorithm gives higher kappa values for short photoperiod groups (kappa above 0.80) than for

long photoperiod groups (kappa below 0.80). It is also expected that the negative influence of light on scoring reliability will be more pronounced in long photoperiod blue-enriched light group. Due to the improvement of the algorithm in detecting REM sleep, a kappa value of around 0.75 is expected for the classification of REM sleep.

Part II: Long-term Effects of Prolonged Photoperiod on Sleep, Wakefulness, and EEG

During prolonged photoperiod, it is hypothesized that total sleep time increases, and that time in wakefulness is reduced, independently of light spectra. Time in SWS is expected to be increased in animals exposed to prolonged photoperiod white light. I expect no changes in SWS time in animals exposed to prolonged photoperiod blue-enriched light. REM sleep is hypothesized to be unchanged as an effect of prolonged photoperiod.

In animals exposed to prolonged photoperiod blue-enriched light, I hypothesize increased beta activity in active wakefulness and reduced beta activity in quiet wakefulness. Slow-wave activity during active phase (rise of Process S) is expected to be reduced in prolonged photoperiod, compared to baseline. A stronger reduction is expected in animals exposed to prolonged photoperiod blue-enriched light. I hypothesize that slow-wave activity in slow-wave sleep (decline of Process S) is reduced during inactive phase in prolonged photoperiod, compared to baseline. I expect that prolonged blue-enriched light exposure will exert an inhibitory effect on slow-wave activity in slow-wave sleep.

These effects are hypothesized to normalize to baseline values in recovery. Compared to the effects of prolonged white light, I expect that the effects of prolonged blue-enriched light will be present for a longer time in recovery. The number of days required to recover will be examined.

2. Methods

2.1. Ethical Approval

This experiment was approved by the Norwegian Animal Research Authority (permit number: 20124636) and performed in accordance with Norwegian laws and regulations controlling experiments in live animals, and The European Convention for the Protection of Vertebrate Animals used for Experimental and Other Scientific Purposes.

2.2. Experimental Design

The total of 12 animals was randomly assigned to one of two experimental groups: prolonged photoperiod white light (n=6), or prolonged photoperiod blue-enriched light (n=6). After surgery and recovery, recordings of sleep (EEG and EMG) and circadian rhythms were carried out in all animals during 5 days of undisturbed baseline, followed by 7 days of exposure to prolonged photoperiod, and 14 days of undisturbed recovery. Figure 4 shows an overview of the design of the experiment.

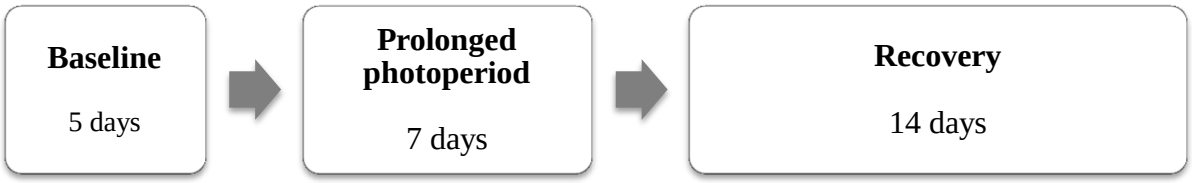

Figure 4. An overview of the experimental design. Sleep (EEG/EMG) was continuously monitored.

2.3. Animals and Housing

Male rats (n=12, Wistar strain, NTac:WH, Taconic, Denmark) were acclimatized to the laboratory conditions upon arrival and group housed in individually ventilated cages (IVC system, Techniplast®, Italy) type IV (480x375x210 mm, 1500cm^2). After surgery, animals were housed individually in IVC cages type III (425x266x185 mm, 800 cm^2). The IVC cages had a ventilation of 75 air changes per hour. Throughout the experiment, temperature was maintained at 23±1°C and the humidity at 40±1%. Animals were fed a standard rodent diet (Rat and mouse no. 1, Special Diets Services, Whitham, Essex, England), and food and water were available *ad libitum*. Except for during the experiment, bedding in cages (BK bedding, Scanbur BK) was changed once a week.

2.3.1. The light dark cycle

In baseline and recovery conditions, animals were kept in a 12:12 light/dark (LD) cycle. Lights went on at 07:00 h (zeitgeber time (ZT) 0), from which they gradually dimmed up until fully on at 08:00 h. At 19:00 h (ZT12), lights gradually dimmed down until fully off at 20:00 h.

During prolonged photoperiod, animals were exposed to 20:4 LD. Here, the lights went off at 03:00 h (ZT20). See figure 5.

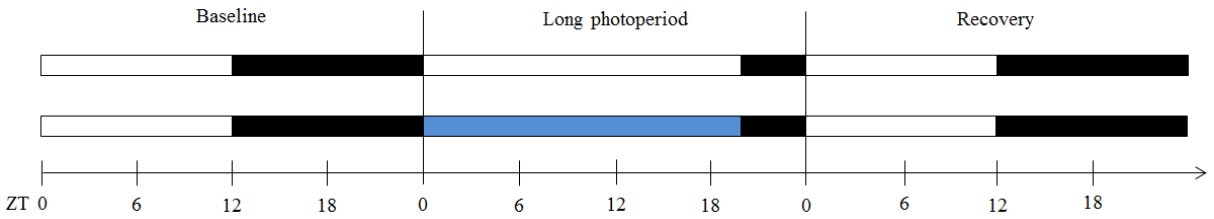

Figure 5. The light dark cycle in baseline, long photoperiod, and recovery. In baseline and recovery, animals were exposed to 12:12 hour light/dark. In long photoperiod, animals were exposed to 20:4 hour light/dark.

2.3.2. Light intensity

Lux (illuminance) and irradiance (intensity of light energy) was measured with GL Spectis 1.0 Touch (GL Optic, Germany). In the white light condition, mean light intensity was 222±112 lux inside cages and the irradiance was 0.8 W/m^2/nm. See figure 6. The blue-enriched light condition included 279±67 lux inside cages and an irradiance of 2.1 W/m^2/nm. See figure 7.

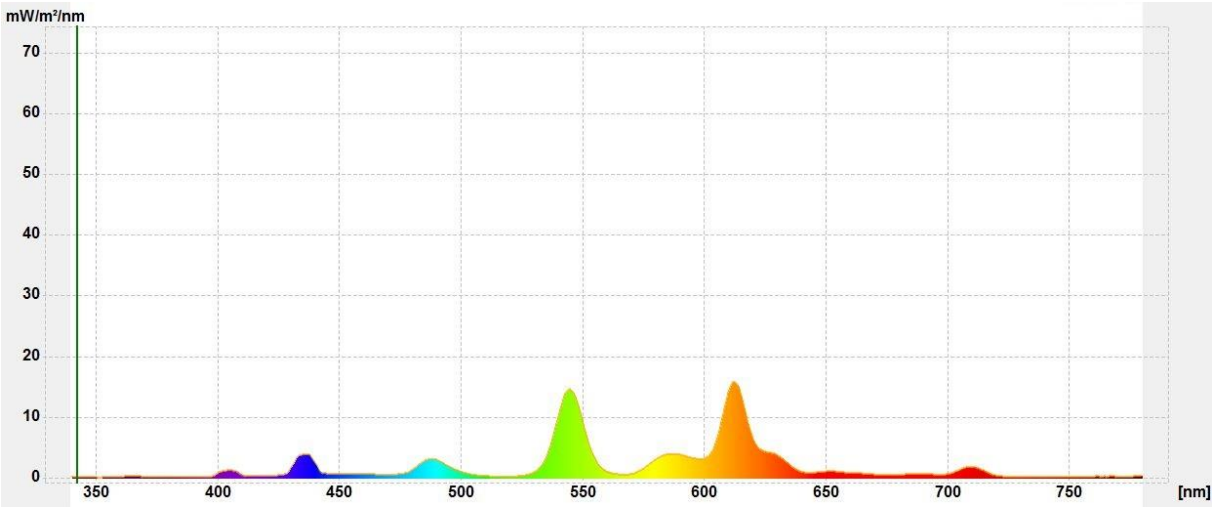

Figure 6. Irradiance spectra for the white light condition, expressed in mW/m^2/nm for each wavelength (nm).

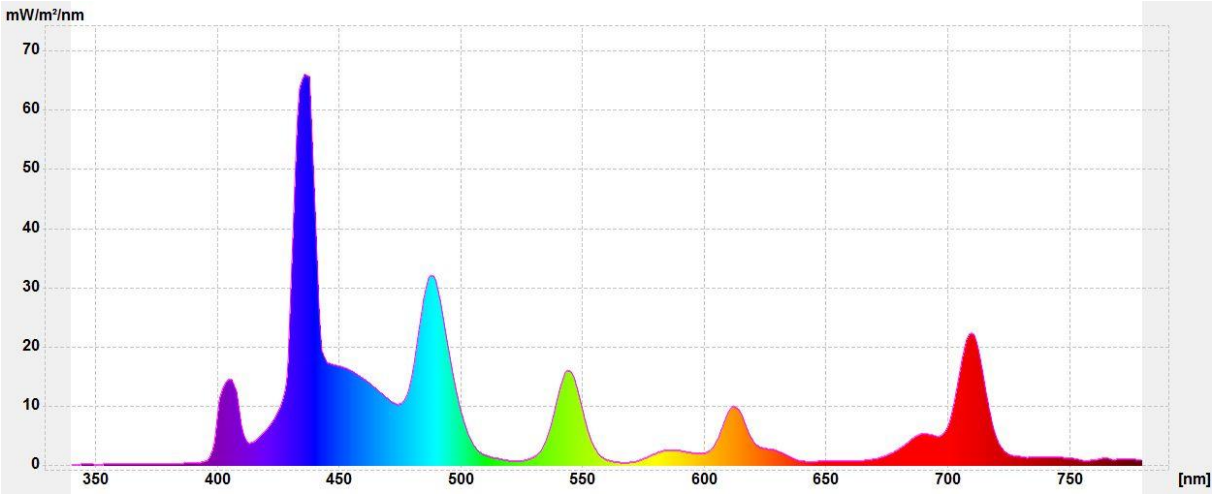

Figure 7. Irradiance spectra for the blue-enriched light condition, expressed in mW/m^2/nm for each wavelength (nm).

2.4. Surgical Procedure

Animals underwent surgery for implantation of transmitters to record continuous and wireless EEG and EMG. Animals were implanted with either one of two telemetric transmitters; F40 or 4ET-S2 (Physiotel®, Data Sciences International, both). Each rat was given antibiotics (trimethoprim, 0.16 mg/ml; sulfamethoxazole, 0.8 mg/ml; Bactrim, Roche) the day before surgery. Anaesthesia for surgery was achieved by giving animals an intraperitoneal (i.p.) injection with a mixture of fentanyl 0.277 mg/kg and medetomidine 0.3 mg/kg (Hypnorm, Janssen; Domitor, Orion). Eye gel (Viscotears®, Novartis) was applied regularly throughout surgery to prevent drying of eyes. Anaesthetized animals were placed in a stereotaxic apparatus (Kopf®, USA) with heating pads laid beneath to maintain normal body temperature. Throughout surgery, the effects of anaesthesia were regularly monitored by testing reflexes of the animal's eye, hind leg and tail. Additional dosage of anaesthesia was given at approximately 45 minute intervals for implantation of frontal-parietal EEG electrodes (bregma coordinates: AP=2.0mm, ML=-2.0mm; lambda coordinates: AP=2.0mm, ML=2.0mm). For the 4ET transmitter, an additional EEG derivation was placed frontal-frontal (bregma coordinates: AP=2.0mm, ML=2.0mm). Frontal and parietal leads were fixed

to the skull using dental acrylic acid (GC RELINE™, America Inc.). Electromyogram (EMG) electrodes were implanted intramuscular, bilaterally in the neck muscle. The sterile telemetric transmitter was implanted in subcutaneous "pocket", in the neck region (F40-EET transmitter) or in the dorsomedial lumbar region (4ET transmitter). Pockets were rinsed with 0.9% sodium chloride (NaCl) and closed with interrupted mattress sutures using re-sorbable thread. Interrupted mattress sutures were used to close skin on the scalp. On the neck and back, skin was closed using clips.

Immediately following surgery, animals were given Ringer's acetate solution (5 ml i.p, Baxter) to compensate for fluid loss during surgery. Analgesic (buprenorphine; 0.30 mg/ml, s.c., Temgesic, Reckit & Benckiser) was administered twice a day the first three post-operative days. Anti-inflammatory agent (meloxicam; 5 mg/ml, s.c., Metacam, Boehringer Ingelheim) was given once a day for three days post-surgery. In addition, antibiotics (trimethoprim, 0.16 mg/ml; sulfamethoxazole, 0.8 mg/ml; Bactrim, Roche) were given in the drinking water the first three post-operative days.

Animals were given a minimum of 14 days to recover from surgery ((Moscardo & Rostello, 2010). Daily care was provided all throughout the post-operative period. Lidocaine liniment (Xylocain, AstraZeneca) and zincbacitracin and chlorhexidine acetate (Bacimycin, Activis) were administered when needed.

2.5. Telemetric Recording

The wireless recording device was calibrated to receive signals in the range from -1.25 to +1.25 mV. To activate the transmitter, a magnet was passed along the side of the animal at the location of the implanted battery. Signals from the telemetric transmitters were collected via receivers (type RPC-2 and RPC-3, Data Sciences International) located beneath the home cage of the animal. EEG and EMG signals were collected at a 250 Hz sampling rate. The

different amplification of the signals (4ET: 240-fold; F40-EET: 200-fold) was corrected for by the use of calibration in the software Dataquest ART. Receivers were connected to a data exchange matrix where signals were converted analogue to digital and transferred to the acquisition software Dataquest ART (version 4.1, Data Sciences International).

2.6. Sleep Analysis Tools

2.6.1. Sleep scoring approach

Sleep was scored using a combination of manual and semi-automatic scoring. Approximately 10% of each sleep recording was manually scored using NeuroScore™ software (version 3.0, Data Sciences International). To assure the subset of manually scored data being representative of the entire recording, epochs were scored across the entire sleep-wake cycle, during lights on and off, and in all experimental conditions. Scoring was performed on unfiltered EEG and EMG signals in 10 s epochs. Manually scored epochs served to train a semi-automatic sleep scoring algorithm (written for MATLAB®, MathWorks, USA) to classify the remaining 90% of epochs in each recording.

2.6.2. Scoring criteria applied by human scorer

A given epoch was assigned the state wakefulness, SWS or REM sleep if the state was present in >50% of the epoch. Wakefulness was scored when EEG displayed high-frequency low-amplitude activity (<80 µV) and EMG activity was moderate-to-high. SWS was scored when there was ≥50% slow wave high-amplitude delta activity (0.5-4 Hz, 250-500 µV) in FP channel or when spindle activity (11-16 Hz, 150-250 µV) was present in FF channel and EMG activity was similar or lower than wakefulness. REM sleep was scored when a

predominant theta activity (6-9 Hz) was present in FP channel and EMG activity was similar or lower than SWS or abolished (muscle atonia).

2.6.3. Semi-automatic sleep scoring algorithm

The scoring algorithm combined two procedures in classifying sleep-wake states: principal component analysis and a näive Bayes classifier (Rempe, Clegern, & Wisor, 2015).

For each manually scored epoch, the algorithm constructed a vector with seven "features" from EEG and EMG power: 1) EEG delta power (1-4 Hz); 2) EEG theta power (5-9 Hz); 3) EEG low beta power (10-20 Hz); 4) EEG high beta power (30-40 Hz); 5) theta-to-delta-ratio; 6) beta-to-delta ratio; and 7) EMG power. Principal component analysis transformed the seven-element feature vector to a new coordinate space where each dimension represents a principal component (PC) and each PC is orthogonal to all of the other PCs. The first three PCs explained over 90% of the variation in the data, therefore only these three were kept. Plotting the data in three dimensional PC space showed clustering of the data according to the sleep state scored.

Using manually scored epochs as training data, a näive Bayes classifier divided the PC space into three distinct "zones" for each state scored (wake, SWS, REM sleep). The classifier performed 10 repeated learning trials on each dataset, using random subsets of 20% of the training data. Each unscored epoch in the recording were subsequently classified according to the clustered zone.

Two contextual rules were included in the classifier: 1) any epoch scored as REM sleep preceded by at least 30 s wake was rescored into wake, and 2) any epoch scored as wake preceded by REM sleep was rescored to REM sleep until there was a significant change in EMG power (1 SD from mean EMG power in the preceding REM sleep episode).

The semi-automatic scoring algorithm calculated five agreement measures, comparing the semi-automatic scoring with the subset (10%) of training data scored by a human: global agreement (% of total epochs scored the same by the machine and a human scorer), wake agreement (number of epochs scored as wake by both the machine and a human, divided by the number of epochs scored as wake by a human), SWS agreement (number of epochs scored as SWS by both the machine and a human, divided by the number of epochs scored as SWS by a human), REM sleep agreement (number of epochs scored as REM sleep by both the machine and a human, divided by the number of epochs scored as REM sleep by a human.

2.6.4. Validation of semi-automatic sleep scoring algorithm

A total of N=20 rat sleep recordings manually scored were included in the validation of the semi-automatic sleep scoring algorithm. The dataset applied in the validation included recordings in four experimental groups of rats: rats in short photoperiod white light (N=4), short photoperiod blue-enriched light (N=4), long photoperiod white light (N=6), and long photoperiod blue-enriched light (N=6). Two scorings per sleep recording were included: one manual scoring (human) and one machine scoring (algorithm). Each recording consisted of 129 600 epochs of 10 s duration.

2.6.4.1. EEG/EMG analysis

The *SLEEP report* app (written for MATLAB®, Mathworks, USA) developed by professor Jonathan Wisor, Washington State University, was used to analyze sleep parameters and EEG power spectral data. The *SLEEP report* app enables a quick and reliable analysis of sleep-wake parameters (in minutes), sleep consolidation parameters (number of bouts and bout duration in minutes) and electrophysiological changes (EEG power in self-defined

frequency bands). The *SLEEP report* app gives flexibility for the interval of interest (for example 360 epochs (1h data) or 8640 epochs (24h data, or any other of interest).

Based on EMG peak-to-peak values, it gives an option to distinguish between two sub states of wakefulness; active wakefulness (AW) and quiet wakefulness (QW). Epochs of QW are defined as EMG≤33rd percentile, whereas wakefulness epochs exhibiting EMG≥66th percentile are reclassified as AW. This criterion is shown to be sufficient to exclude epochs with high locomotor activity from QW and demonstrate unique electrophysiological changes between QW and AW, across frequency bands and cortices (Grønli, Janne, Rempe, et al., 2016).

Moreover, power spectral analysis is performed by Fast Fourier Transform (FFT) analysis on unfiltered EEG signals on each 10-sec epoch segregated into 2-sec intervals with a Hamming window and 50% overlap, yielding an average power value for the 10-sec epoch. Artefacts are removed in the *SLEEP report* app by detecting epochs with values exceeding the mean value x 8 SDs. EEG power bands included in the present analysis were defined as Delta 1-4 Hz, Theta 5-8 Hz, Alpha 9-12 Hz, and Beta 15-30 Hz.

2.6.4.2. Mathematical modeling of the rise and decline of process S

An advantage of the scientific field of basic sleep research is that the homeostatic regulation of sleep can be expressed mathematically. A homeostatic model of sleep was applied to quantify the time dynamics (rates) at which process S rises and declines in prolonged photoperiod and the recovery phase, compared to baseline. The model is based on the modeling framework in Rempe & Wisor (2014) and has recently been tested on data in a rodent model of shift work (Rempe et al. in press). In order to quantify the time dynamics in process S, the model first found all overlapping segments in the EEG that were of 5 minute duration and consisted of ≥90% SWS. In these segments, the model computed mean EEG

delta power (SWA; 1-4 Hz), and the computed SWA-value for each segment was fitted to a homeostatic model in where SWA rose during epochs scored as wakefulness or REM sleep and declined during epochs scored as SWS. The rates at which process S rose and declined during wakefulness or REM sleep, and during SWS, were quantified with the following equations:

$$S_{t+1} = UA - (UA - S_t)e^{\frac{-\Delta t}{Ti}} \quad \textbf{Wakefulness or REM sleep}$$

$$S_{t+1} = LA + (S_t - LA)e^{\frac{-\Delta t}{Td}} \quad \textbf{SWS}$$

The upper asymptote (UA) represents the 99% level of SWA distribution during SWS, and the lower asymptote (LA) represents the intersection of SWA histogram curves during REM sleep and SWS. Ti represents the rising time constant, and Td represents the declining time constant of process S. Ti and Td are the only parameters in the equations that are free to vary (the rest of the parameters are fixed values found for each recording). In the homeostatic model, Ti and Td were fit individually to each EEG recording and the values of Ti and Td were optimized for baseline, day 7 of exposure to prolonged photoperiod, and during the recovery days 1, 3, 5 and 7.

2.7. Statistical Analyses

The reliability of semi-automatic sleep scoring algorithm was determined by the use of a MATLAB® script (Mathworks, USA) made by Hanne Siri Amdahl Heglum, Norwegian University of Science and Technology, and Novelda AS. Here, all epochs manually scored were compared with the corresponding epochs of the machine scoring. The reliability of the semi-automatic scoring was determined by 1) overall percentage agreement (measure of

consistency among scorers; the percentage of total epochs in agreement between the machine and the human scorer), and 2) Cohen's unweighted kappa (κ) coefficient as an index of inter-rater reliability for each sleep-wake state.

Cohen's κ is a correlation coefficient ranging from -1 to 1 that quantifies agreement between two scorers while accounting for agreement occurring by chance (Cohen, 1960) formula used: $1-((1-P_0)/(1-P_e))$ where P_0 is the observed proportional agreement between manual and machine scoring, and P_e is the hypothetical probability of chance agreement between manual and machine scoring). The most widely cited interpretation of Cohen's κ is that of Landis and Koch: <0.00 poor agreement, 0.00-0.20 slight agreement, 0.21-0.40 fair agreement, 0.41-0.60 moderate agreement, 0.61-0.80 substantial agreement, 0.81-1.00 almost perfect agreement (Landis & Koch, 1977). Semi-automatic scorings returning a κ value <0.81 were manually rescored.

Overall agreement in undisturbed condition were compared to the experimental groups using Student's *t*-test (two-tailed).

All statistical analyses addressing our second aim for the effect of prolonged photoperiod were conducted using Statistica™ (version 13.3, TIBCO® Software Inc). The two 'light' conditions (white and blue-enriched) were classified as independent factors. One-way analysis of variance (ANOVA) was used to ensure that the two conditions did not differ in any parameters in baseline. To test any experimental effects in 1) prolonged photoperiod and 2) reocvery, 'days' was classified as dependent variables and analysed using ANOVA for repeated measures with factorial design. The dependent variable 'days' during 1) prolonged photoperiod were baseline and E7, and 2) during recovery: baseline, R1, R3, R5 and R7. Repeated measure ANOVA was used for a) sleep parameters (TST, SWS, REM sleep, wakefulness, active wakefulness and quiet wakefulness) , b) sleep consolidation measures (number and duration of wake bouts, SWS bouts and REM sleep bouts), c)

electrophysiological measures (SWA in SWS and beta activity during quiet wakefulness) and d) output parameters from mathematical modelling of process S (Ti, the rising time constant of process S; UA, the upper asymptote of the rise; Td, the declining time constant of process S; and LA, the lower asymptote of the decline).

The homeostatic regulation of sleep (decline in SWA during SWS) was assessed by repeated measures ANOVA with 'light' (white and blue-enriched) classified as independent factors, 'days' (baseline/E7 and baseline/R1/R3/R5/R7) and 'ZT' (ZT0, ZT2, ZT5, ZT11) classified as dependent variables.

All significant overall effects of ANOVA were followed-up with Fisher's LSD *post hoc* test. Significance was accepted at $p \leq 0.05$. Cohen's d was calculated for between-light group comparisons (M1-M2)/SD pooled) and for within-light group comparisons ((M1-M2)/((√($sd1^2$+$sd2^2$))*(-1)) as an estimation of effect size. By convention, an effect size of 0.2 is considered small, around 0.5 is considered a medium effect and 0.8 and above is considered a large effect (Cohen, 1992). Positive d values represent increase and negative values represent decrease in one group relative to another. Different degrees of freedom in the results section are due to exclusion of some animals from analysis when showing values more than 2 standard deviations from the group mean. One animal from white light condition was excluded from statistical analyses on the decline in SWA during SWS in experimental condition and recovery period due to extensive artefacts in the EEG. One animal from white light condition was excluded from statistical analyses on mathematical modelling output in the recovery phase due to failed modeling. All results are presented as mean ± SEM.

3. Results

3.1. Part 1: Validation of a Semi-automatic Sleep Scoring Algorithm compared to a Gold Standard

Table 1

Performance of machine relative to human scoring in baseline and four experimental groups, assessed by overall agreement, Cohen's unweighted kappa coefficient for wake, SWS, and REMS.

Experimental group	Overall agreement (%)	Kappa		
		Wake	SWS	REMS
Baseline	84.85±2.38	0.73±0.04	0.75±0.04	0.78±0.04
SW	90.57±0.95	0.82±0.02	0.86±0.02	0.85±0.02
SB	87.38±1.82	0.76±0.03	0.82±0.02	0.76±0.06
LW	82.70±4.01	0.69±0.07	0.71±0.07	0.77±0.05
LB	83.72±3.79	0.69±0.07	0.74±0.07	0.78±0.03

Overall agreement and Cohen's unweighted kappa coefficient is listed as mean±standard error of the mean.
Bolded numbers indicate mean kappa values meeting the criteria of 'almost perfect agreement'.
Abbreviations: SW *short* photoperiod *white* light; SB *short* photoperiod *blue-enriched* light; LW *long* photoperiod *white* light; LB *long* photoperiod *blue-enriched* light, SWS slow-wave sleep; REMS rapid eye movement sleep

In undisturbed animals (n=20), the overall agreement between machine and manual scoring was 84.8 ± 2.4%. Thus, in approximately 85% of all epochs, machine and human scorer agreed on classifying an epoch either as wake, SWS or REM sleep. Mean inter-rater reliability (indexed by Cohen's κ) between machine and manual scoring in classifying the sleep-wake states showed a substantial agreement (0.73 to 0.78).

3.1.1. Performance of a semi-automatic sleep scoring algorithm in four experimental groups

A summary of the results of inter-rater reliability is presented in Table 1.

a) Short photoperiod white light (4:20 LD). Overall agreement between machine and manual scoring was higher than in undisturbed animals, 90.6 ± 1.0%, p=0.04. Inter-rater reliability showed almost perfect agreement (0.82 to 0.86).

b) Short photoperiod blue-enriched light (4:20 LD). Overall agreement was similar to undisturbed animals, 87.4 ± 1.8%, p=0.41. The inter-rater reliability between machine and manual scoring was substantial to almost perfect (0.76 to 0.82).

c) Long photoperiod white light (20:4 LD). Overall agreement was similar to undisturbed animals 82.7 ± 4.0%, p=0.66. The inter-rater reliability showed substantial agreement (0.69 to 0.77).

d) Long photoperiod blue-enriched light (20:4 LD). Overall agreement between machine and manual scoring was similar to undisturbed animals 83.7 ± 3.8%, p=0.81. The inter-rater reliability showed substantial agreement (0.69 to 0.78).

3.2. Part 2: Long-term effects of prolonged photoperiod on sleep-wake dynamics, electroencephalographic changes and the homeostatic regulation of sleep

A summary of the results with statistical main effects is presented in Appendix A, Table I and II.

3.2.1. Baseline analyses (12:12 LD)

The two groups did not differ in any of the sleep or electrophysiological parameters during baseline (light; $F_{(1,10)}$'s≤2.44, p's≥0.149). All rats displayed a rhythmic and polyphasic sleep-wakefulness pattern characteristic of nocturnal rodents. Sleep predominated during the light (L) phase (54% SWS, 15% REM sleep and 31% wakefulness). Wakefulness predominated during the dark (D) phase (24% SWS, 4% REM sleep and 72% wakefulness).

3.2.2. Homeostatic sleep regulation during baseline

In baseline, the SWA in SWS declined during the L phase (ZT; $F_{(4,40)}$=17.27, p>0.001), similarly in both light conditions (light; $F_{(1,10)}$=1.53, p=0.244). The reduction in sleep pressure was characterized by a significant decline in SWA from ZT0 to ZT2 (p=0.002) and from ZT2 to ZT5 (p=0.016). None of the parameters of the mathematical modeling of process S (Ti, UA, Td and LA) differed between groups (light; $F_{(1,10)}$'s≤1.97, p's>0.05).

3.2.3. Long-term effects of prolonged photoperiod

A summary of the results with statistical main and interaction effects are presented in Appendix B, Table III and IIII.

After 7 days (E7) in prolonged photoperiod, there was an effect of day on several parameters of sleep and sleep consolidation (days: $F_{(1,10)}$'s ≥6.62, p's>0.05,). Independently of light spectra, there was an increase in TST (p=0.004; white: +8.9% and blue-enriched: +3.6%) and time spent in SWS (p=0.011; white: +8.9% and blue-enriched: +4.1%), while time spent in wakefulness was reduced (p=0.004; white: - 7.4% and blue-enriched: - 3.8%) compared to baseline (Figure 8).

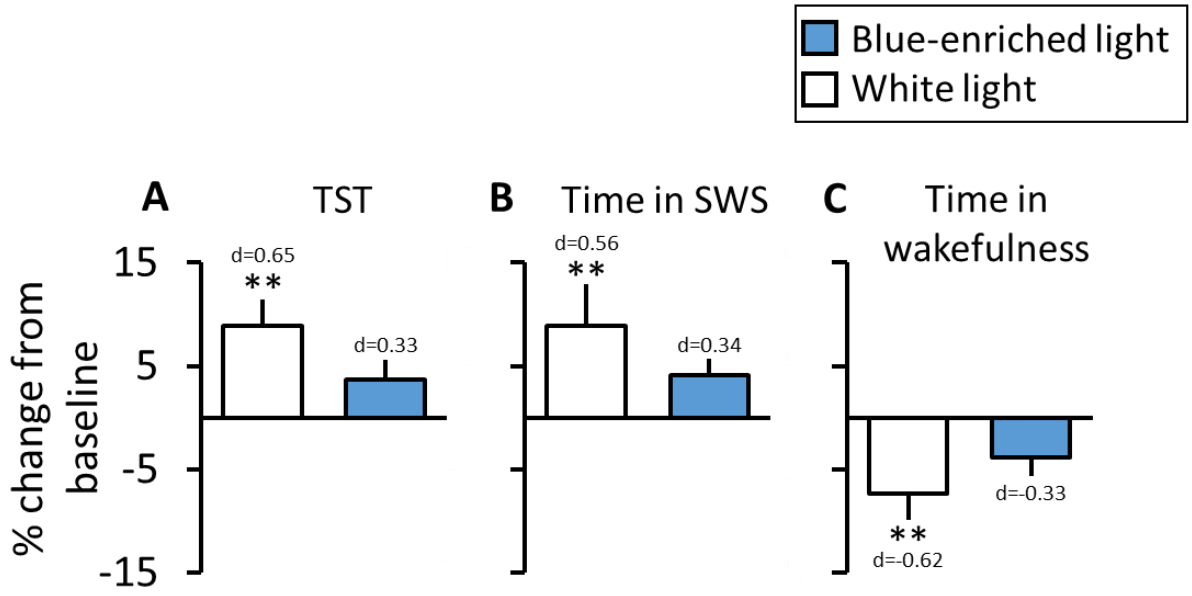

Figure 8. Long-term effects of prolonged photoperiod on sleep and wakefulness, at exposure day 7 of 20:4 LD, in white (white bars) or blue-enriched (blue bars) light. A) Total sleep time (TST), B) Time in slow-wave sleep (SWS), C) Time in wakefulness. Data is shown as mean % change from 12:12 LD baseline. Error bars indicate SEM. Asterisks indicate significant differences compared to baseline; ** $p \leq 0.01$. d indicates Cohen's d compared to baseline; ≤0.5 small effect size and 0.5-0.8 medium effect size.

Consolidation of sleep was increased after 7 days in prolonged photoperiod. Number of SWS and REM sleep bouts were longer (SWS: p=0.017; white: +13.4% and blue-enriched: +17.8%; REM sleep: p=0.021; white: + 23.0% and blue-enriched: +5.4%), and wake bout duration was shorter p=0.005: white: - 15.2% and blue-enriched: - 19.1%) (Figure 9).

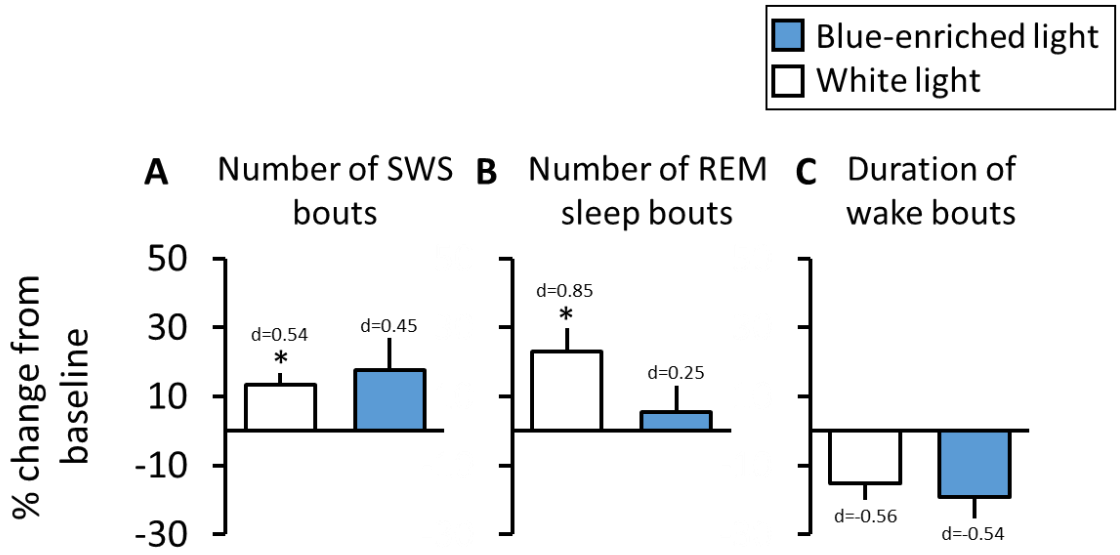

Figure 9. Long-term effects of prolonged photoperiod on sleep and wake bouts, at exposure day 7 of 20:4 LD, in white (white bars) or blue-enriched (blue bars) light. A) number of slow wave sleep (SWS) bouts, B) number of REM sleep bouts, C) Duration of wake bouts. Data is shown as mean % change from 12:12 LD baseline. Error bars indicate SEM. Asterisks indicate significant differences compared to baseline; * $p \leq 0.05$. d indicates Cohen's d compared to baseline; ≤0.5 small effect size, 0.5-0.8 medium effect size, ≥0.8 large effect size.

No other parameters on sleep and wakefulness were significantly affected at E7 compared to baseline ($F_{(1,10)}$'s≤5.24, p's>0.05).

3.2.4. Electrophysiological changes during SWS and quiet wakefulness

SWA in SWS showed no significant main or interaction effects ($F_{(1,10)}$'s≤0.72, p's>0.42).

Beta activity in quiet wakefulness showed an interaction effect between day and light ($F_{(1,10)}$=9.57, p=0.01), where blue-enriched light suppressed beta activity compared to baseline (-10.6±2.5%, p=0.003) This was not evident in the white light condition (10.2±8.5%, p=0.599) (Figure 10A). There was no effect on beta activity during active wakefulness (Figure 10B).

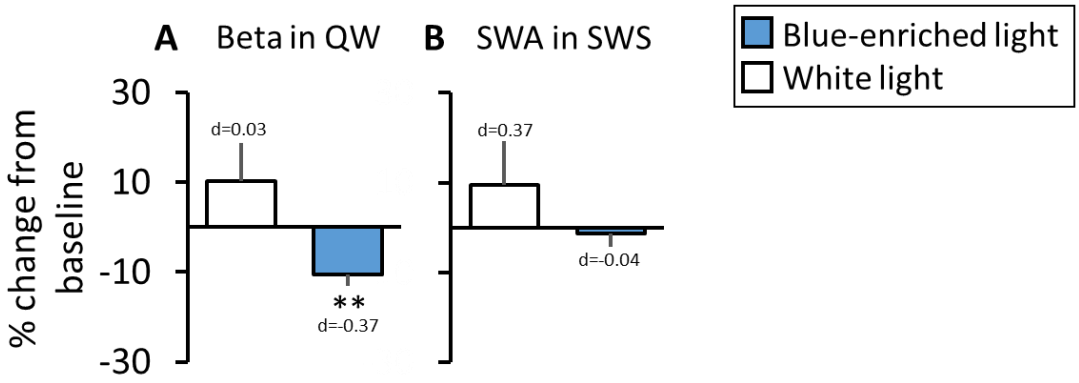

Figure 10. Long-term effects of prolonged photoperiod on electrophysiological changes in sleep and wakefulness, at exposure day 7 of 20:4 LD, in white (white bars) or blue-enriched (blue bars) light. A) Slow wave activity (SWA) in slow wave sleep (SWS), B) Beta in quiet wake (QW). Data is shown as mean % change from 12:12 LD baseline. Error bars indicate SEM. Asterisks indicate significant differences compared to baseline; ** $p \leq 0.01$. d indicates Cohen's d compared to baseline; ≤0.5 small effect size.

3.2.5. Homeostatic sleep regulation

During L, SWA in SWS showed a main effect of ZT ($F_{(3,27)}$=24.37, p<0.001) and interaction effect between day and ZT ($F_{(3,27)}$=3.94, p=0.019). Independent of light spectra, homeostatic sleep pressure declined from ZT0 to ZT2 (p<0.001). See Figure 11.

The SWA at the different ZTs was similar to baseline recording at ZT0 throughout ZT5 (p's>0.05). At ZT11, the SWA was higher than baseline (p=0.004; white: *d*= 1.75 and blue-enriched: *d*= 0.80). See Figure 11.

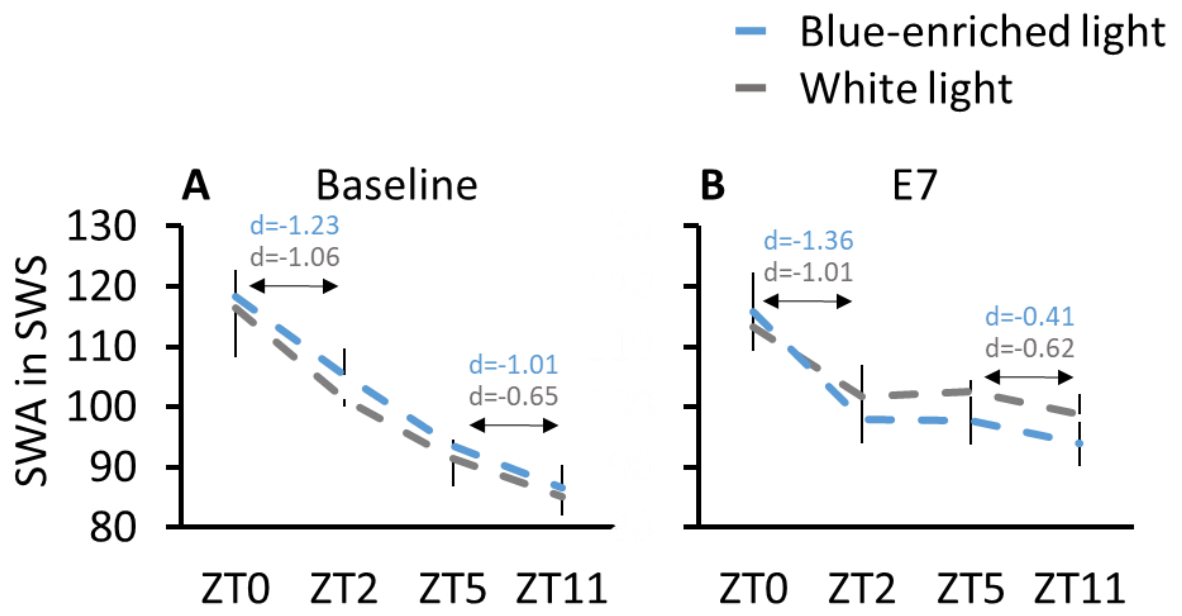

Figure 11. Reduction in sleep pressure (slow wave activity, SWA, in slow wave sleep, SWS) across zeitgeber time 0-11 (ZT0-11), during A) 12:12 LD baseline, and B) exposure day 7 (E7) in white (grey line) or blue-enriched (blue line) light. Error bars indicate SEM. d indicates Cohen's d between time-points indicated by arrows (ZT0 zs ZT2 and ZT5 vs ZT11); ≤0.5 small effect size, 0.5-0.8 medium effect size, ≥0.8 large effect size.

None of the parameters of the mathematical modeling of process S (Ti, UA, Td and LA) were significantly different after prolonged photoperiod ($F_{(1.10)}$'s≤4.66, p's>0.05).

3.3. Part III: Recovery from Prolonged Photoperiod

An overview of the results with statistical main effects and interaction effects is presented in Appendix C, Table V-VI.

In the recovery period, there was an effect of day on several parameters of sleep and sleep consolidation ($F_{(4,40)}$'s≥2.54, p's<0.05,). Sleep parameters were affected at R3 only and independently of the prior exposure to different light spectra. Here, TST was longer (p=0.047; white: +2.7% and blue-enriched: +8.3) compared to baseline. Time in wakefulness was shorter (p=0.049; white: -2.6% and blue-enriched: -7.7%), where the time in active

wakefulness was reduced in particular (p=0.004; white: -10.3% and blue-enriched: -9.8%) compared to baseline (Figure 12).

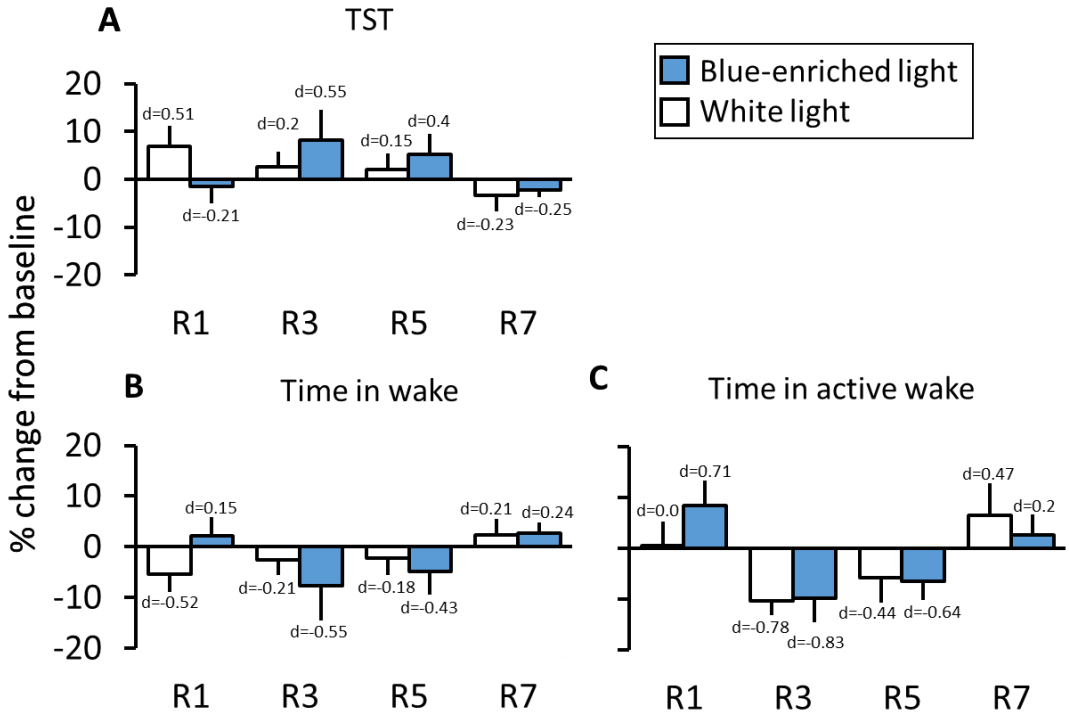

Figure 12. Sleep and wake parameters during 12:12 LD recovery, following 7d of 20:4 LD, in white (white bars) or blue-enriched (blue bars) light. Recovery days 1, 3, 5 and 7 (R1, R2, R3, R7). A) Total sleep time (TST), B) Time in wakefulness, C) Time in active wakefulness. Data is shown as mean % change from 12:12 LD baseline. Error bars indicate SEM. d indicates Cohen's d compared to baseline; ≤0.5 small effect size, 0.5-0.8 medium effect size, ≥0.8 large effect size.

Parameters reflecting sleep consolidation was more affected in the recovery from prolonged photoperiod. There were more SWS bouts, both at R3 (p=0.001; white: +8.2% and blue-enriched: +18.7) and R5 (p=0.017; white: +6.9% and blue-enriched: +13.7%) compared to baseline. There were more REM sleep bouts both at R1 (p=0.036; white: +17.9% and blue-enriched: +4.5%), R3 (p<0.001; white: +23.2% and blue-enriched: +15.7) and R5 (p=0.036; white: +12.5% and blue-enriched: +10.8%). The wake bouts were shorter at R3 (p<0.001,

white: -12.9% and blue-enriched: -19.1%) and at R5 (p=0.009, white: -4.4% and blue-enriched: -16.9%). See Figure 13.

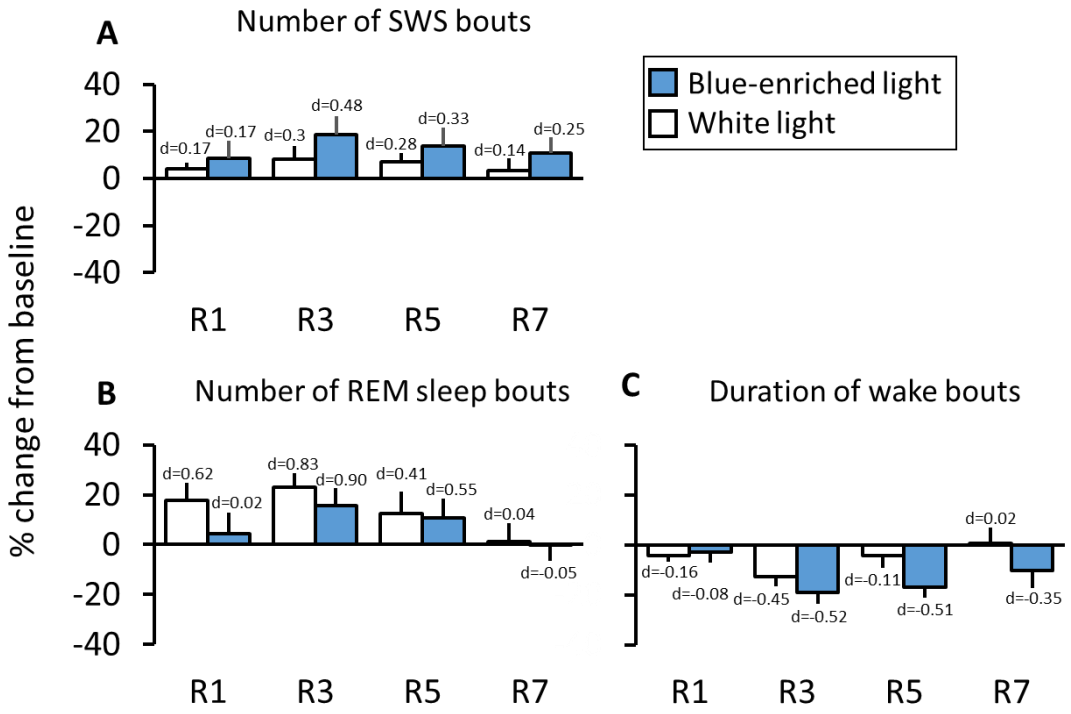

Figure 13. Sleep and wake bout parameters during 12:12 LD recovery, following 7d of 20:4 LD, in white (white bars) or blue-enriched (blue bars) light. Recovery days 1, 3, 5 and 7 (R1, R2, R3, R7). A) Number of slow wave sleep (SWS) bouts, B) Number of REM sleep bouts, C) Duration of wake bouts. Data is shown as mean % change from 12:12 LD baseline. Error bars indicate SEM. d indicates Cohen's d compared to baseline; ≤0.5 small effect size, 0.5-0.8 medium effect size, ≥0.8 large effect size.

3.3.1. Electrophysiological changes during quiet wakefulness and SWS

SWA in SWS showed no significant main or interaction effects ($F_{(4,40)}$'s≤0.77, p's>0.40).

There was an interaction effect between days and light ($F_{(4,40)}$=6.13, p<0.001) on beta activity in quiet wakefulness. Prior exposure to blue-enriched light suppressed beta activity in

quiet wakefulness throughout the recovery period compared to baseline; R1 (-5.8±2.4%, p=0.008), R3 (-7.9±3.2%, p<0.001), R5 (-11.5±4.7%, p<0.001), and R7 (-9.4±3.8%, p<0.001). There was no such suppression in recovery from the white light condition (p's>0.05). See Figure 14.

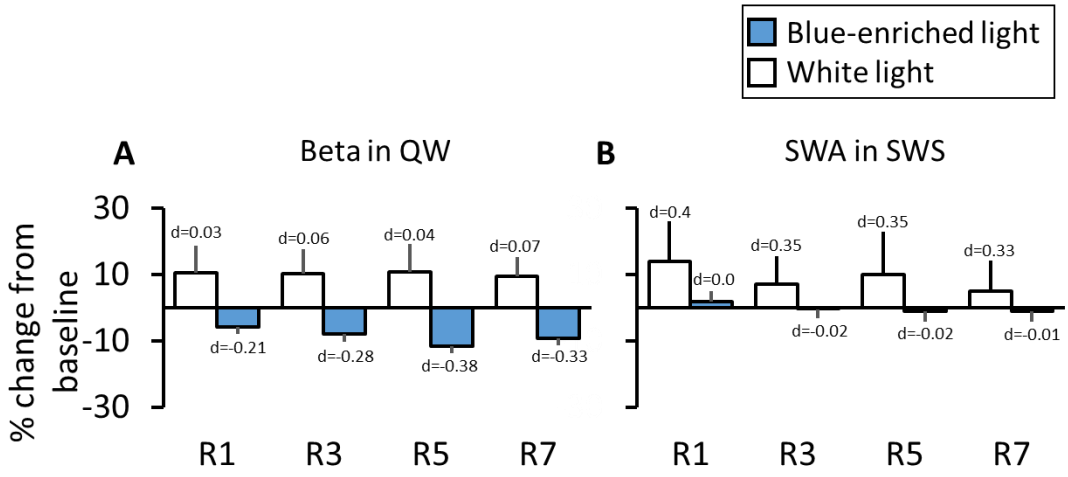

Figure 14. Electrophysiological changes during 12:12 LD recovery, following 7d of 20:4 LD, in white (white bars) or blue-enriched (blue bars) light. Recovery days 1, 3, 5 and 7 (R1, R2, R3, R7). A) Beta in quiet wake (QW), B) Slow wave activity (SWA) in slow wave sleep (SWS). Data is shown as mean % change from 12:12 LD baseline. Error bars indicate SEM. d indicates Cohen's d compared to baseline; ≤0.5 small effect size.

No other sleep, wakefulness or EEG parameters were significantly affected in recovery compared to baseline ($F_{(4,40)}$'s≤1.98, p's>0.05).

3.3.2. Homeostatic sleep regulation

In the recovery from prolonged photoperiod there was a main effect of days ($F_{(4,36)}$=6.62, p<0.001) and ZT ($F_{(3,27)}$=32.04, p<0.001), and an interaction effect between days and ZT ($F_{(12,108)}$=2.30, p=0.012).

The decline in homeostatic sleep pressure differed during the recovery period. SWA in SWS declined at R1 from ZT0 to ZT2 (p<0.001), at R3 and R5 from ZT5 to ZT11 (p=0.039

and p=0.046, respectively), and at R7 from ZT0 to ZT2 (p=0.032) and ZT5 to ZT11 (p=0.049). See Figure 15.

The SWA at the different ZTs contrasted baseline recording in a different pattern across the recovery period. At R1 SWA differed at ZT5 (p=0.005: white, *d*= 1.56; blue-enriched: *d*= 1.94) and ZT11 (p=0.003: white, *d*= 2.03; blue-enriched: *d*= 1.22). At R3 SWA differed at ZT0 (p=0.003: white, *d*= -1.09; blue-enriched: *d*= -0.60), ZT5 (p=0.043: white, *d*= 0.25; blue-enriched: *d*= 1.63) and ZT11 (p=0.012: white, *d*= 1.43; blue-enriched: *d*= 0.79). At R5 and R7 SWA differed at ZT0 (R5: p=0.003: white, *d*= -1.21; blue-enriched: *d*= -0.61; and R7: p=0.003: white, *d*= -0.70; blue-enriched: *d*= -0.61).

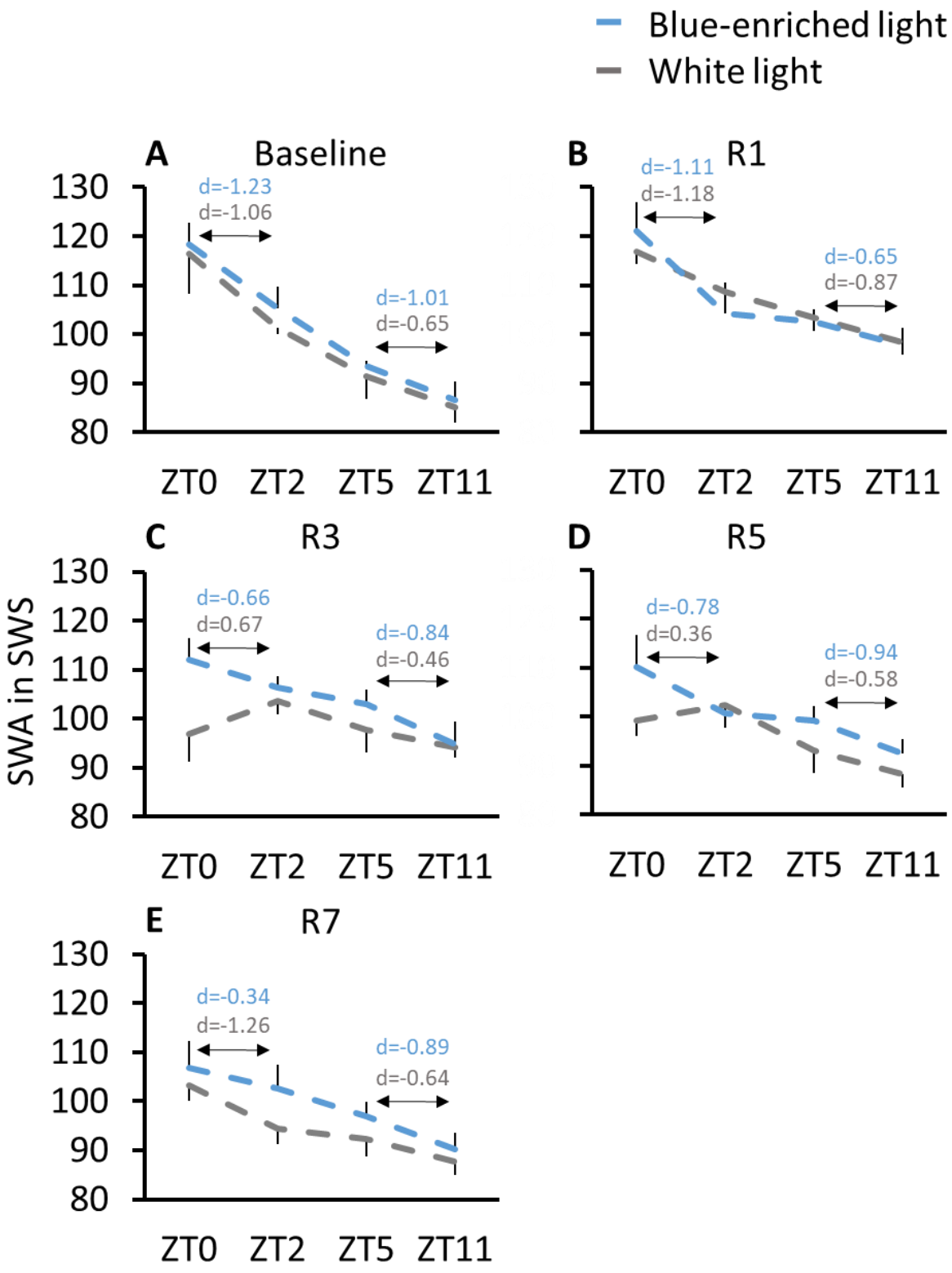

Figure 15. Reduction in sleep pressure (slow wave activity, SWA, in slow wave sleep, SWS) across zeitgeber time 0-11 (ZT0-11), during baseline and recovery from 7d 20:4 LD in white (grey line) or blue-enriched (blue line) light. A) 12:12 LD baseline, B) Recovery day 1 (R1), C) R3, D) R5, E) R7. Error bars indicate SEM. d

indicates Cohen's d between time-points indicated by arrows (ZT0 zs ZT2 and ZT5 vs ZT11); ≤0.5 small effect size, 0.5-0.8 medium effect size, ≥0.8 large effect size.

3.3.3. Mathematical modeling of process S

None of the parameters (Ti, UA, Td and LA) of the mathematical modeling of process S showed an effect of days, light or interaction thereof ($F_{(1.10)}$'s≤4.66, p's>0.05).

4. Discussion

The aims of this study were to 1) validate a semi-automatic sleep scoring algorithm in rats exposed to various photoperiodic manipulations, and 2) characterize the long-term effects of prolonged photoperiod on sleep-wake dynamics, including sleep timing, sleep consolidation, electrophysiological changes, and homeostatic sleep regulation in rats.

In the first part of the discussion I will discuss the performance of the semi-automatic algorithm in relation to the performance of other (semi-) automatic sleep scoring algorithms developed for rodent sleep, and across different experimental conditions.

Second, results from the rat model of prolonged photoperiod (20:4 LD) show that 7 days of exposure to prolonged photoperiod induces differential effects on sleep-wake dynamics, electrophysiological changes, and homeostatic sleep regulation, dependent upon spectral intensity. I will discuss these findings in relation to a) studies examining how light of different spectral intensities affect sleep and arousal – and hypotheses and models put forward in an attempt to explain these effects through projections from the intrinsic photosensitive ganglion cells of the retina (ipRGCs), and b) process S in the two-process model of sleep regulation.

4.1. Part I: Validation of a semi-automatic sleep scoring algorithm compared to a Gold Standard

My study evaluated the accuracy of a semi-automatic algorithm developed to score sleep stages in rodents, compared to manual gold scoring. The gold standard in my study was three human scorers, all highly trained and experienced in the scoring of rodent sleep. Two of them were also highly trained in scoring human sleep. We all agreed on the gold standard applied, based on scoring criteria developed in Bergen Stress and Sleep Group (see 'Sleep stages in rats').

The main finding in my study was that the semi-automatic sleep scoring algorithm was comparable to manual scoring for all stages. The kappa coefficient (κ) between the semi-automatic sleep scoring algorithm and the gold standard was substantial in the classification for both wakefulness, SWS and REM sleep (κ = 0.74, 0.78 and 0.79, respectively). The overall agreement between the semi-automatic algorithm and manual gold scoring was strong; approximately 85%.

In experimental conditions which included changes in the light condition (hours with light and/or light spectra), the algorithm performed better (91%) in the experimental conditions where the light phase (inactive period) was short. However, this was dependent on the light spectra, and only for white light (κ = 0.85 to 0.88). The algorithm performed similar to the undisturbed condition when the light phase was long, and in both blue-enriched conditions (overall agreement = 83 to 87% and κ = 0.72 to 0.80).

My validation study utilized two indexes to quantify the agreement between semi-automatic and manual scoring: overall agreement and the kappa coefficient (κ), an index of inter-rater reliability. The semi-automatic sleep scoring algorithm was comparable to manual scoring for classification of all three states; wakefulness, SWS and REM sleep. There

was a strong overall agreement (87%) and the κ coefficient for wakefulness, SWS and REM sleep was 0.74, 0.78 and 0.79, respectively.

In the past 10 years several research laboratories have published results from studies examining the performance of (semi-)automated sleep scoring algorithms developed for mice and rats (Bastianini et al., 2014; Gilmour, Fang, Guan, & Subramanian, 2010; Libourel, Corneyllie, Luppi, Chouvet, & Gervasoni, 2015; Rytkönen, Zitting, & Porkka-Heiskanen, 2011). It should be noted that some of these (e.g. Bastianini et al., 2014; Rytkonen et al, 2011) do not report κ coefficients as a quantification of state-specific agreement. Rather they provide information on the accuracy, sensitivity and specificity of the algorithm employed. The numbers of accuracy, sensitivity and specificity are not comparable to those of κ coefficients due to the fact that the κ coefficient takes random agreement between scorers into account. Thus, the level of agreement is reduced compared to calculations not taking random agreement into account (such as those of accuracy, sensitivity and specificity).

Gilmour and colleagues (2010), reported to reach a better overall agreement of 94-95% and better κ = 0.89 to 0.91, than our algorithm. Whereas, other algorithms perform poorer (83% overall agreement and κ approaching 0.78 in Libourel et al. (2015)). In Rytkonen et al. (2011), the sensitivity and specificity for wakefulness was 94% and 96%, 94% and 97% for SWS, and 89% and 97% for REM sleep, respectively. Although the overall agreement for this algorithm was better than that in our algorithm, the hypothetical κ values (had Rytkonen reported these) would much likely have been substantially lower than those reported in this validation study.

Light is a factor that disrupts sleep architecture and influences scoring reliability, yet it had limited impact on the difficulty of the semi-automatic algorithm in classifying wakefulness, SWS and REM sleep. When examining the sensitivity of the semi-automatic algorithm to the experimental condition of short photoperiod (shorter inactive phase), the

overall agreement were similar or improved compared to baseline (baseline: 85%; short white: 91%; short blue-enriched: 87%). For the experimental condition of prolonged photoperiod (longer inactive phase), the agreement markedly weakened (long white: 83% and long blue-enriched: 84%). Short photoperiod, independent of light spectra, improves auto-staged detection of SWS (baseline: 0.75; short white: 0.86; short blue-enriched: 0.82) and wakefulness (baseline: 0.73; short white: 0.82; short blue-enriched: 0.76). This may be explained by easier-to-recognize signal patterns.

Not only does light in general influence scoring reliability in terms of improved sensitivity in detection of SWS and wakefulness (if short photoperiod), also limited light hours may strengthen the reliability of semi-automated sleep state classification. If long photoperiod, wakefulness, SWS and REM sleep were scored fairly similarly compared to undisturbed condition. Hence, the energy imparted by photons of blue wavelengths which has been shown to suppress EEG delta power in SWS and induce alertness did not make it more difficult to detect the stages of SWS and wakefulness. In the detection of SWS, the semi-automatic sleep scoring algorithm assesses the magnitude differences (ratios) in delta and theta power spectral density. Manual scoring, on the other hand, relies on EEG amplitude in the detection of SWS. EEG amplitude is influenced by a range of factors, e.g. the distance between the active and inactive electrode, thickness of the skull, and individual differences in neurobiology. Thus, semi-automatic scoring algorithm applies a broader and more consistent approach to stage EEG signals.

In addition to altered sleep staging sensitivity due to experimental conditions, the quality of the EEG signal is also an important factor influencing how well the semi-automatic sleep scoring algorithm is able to differentiate between sleep-wake states. A noisy signal (e.g. due to large positive or negative signal deflections) makes it more difficult to differentiate between SWS and wakefulness.

A common observation in sleep scoring is that of low inter-rater agreement for REM sleep, irrespective of manual or machine-based scoring. A previous version of the semi-automatic algorithm being validated here was specifically developed to increase the accuracy of REM sleep detection. This was done partly by adding rules from the AASM manual for human sleep scoring (Berry et al., 2012). The fifth rule for scoring REM sleep in humans ("*Continue to score segments of sleep that follow one or more definite stage REM sleep as stage REM sleep if the EMG tone is low for the majority of the epoch"*) was applied to the semi-automatic sleep scoring algorithm in the sense that, any epoch scored as wakefulness preceded by REM sleep was rescored into REM sleep until there was a significant change in EMG power (1 SD from mean EMG power of the preceding REM sleep episode). A stage characterized by active REM sleep is somewhat similar to signals present in the state of wakefulness. To avoid the misclassification of wakefulness epochs as REM epochs, a rule was added to rescore REM sleep into wakefulness if the given epoch was preceded by at least 30 s of wakefulness. The semi-automatic sleep scoring algorithm was also improved in terms of the avoidance of artefacts exceeding 8 SDs above the mean. These modifications resulted in better performance in the detection of REM sleep than wakefulness and SWS (κ =0.79 for REM sleep vs. 0.74 for wakefulness and 0.78 for SWS). This is in contrast to the performance of other sleep scoring algorithms in where the detection of wakefulness and SWS outperforms the detection of REM sleep (Bastianini et al., 2014; Gilmour et al., 2010; Rytkönen et al., 2011).

Although we eased the use of time doing a full manual scoring by employing a semi-automatic sleep algorithm to score the data, we observed that it was necessary to re-score the output from the experimental condition of prolonged photoperiod both in white and blue-enriched light conditions. However, our semi-automatic sleep scoring algorithm displayed considerably good agreement with the gold standard (85%), and thus, by using an effective

algorithm displaying a high level of inter-rater agreement, the human scorer is allowed to focus on spending more time on the notoriously difficult stage transitions, such as from REM sleep to wakefulness, and from wakefulness to SWS.

The development and improvement of semi-automatic sleep-wake classification algorithms, such as those discussed in this validation study, is important in order to reduce the probability of scoring errors within the same scorer but also to increase the degree of inter-rater reliability between scorers in the same laboratory and between scorers across laboratories. The latter is of special importance due to the fact that a standardized scoring manual for rodent sleep is yet to be published.

4.2. Part II Long-term effects of prolonged photoperiod on sleep-wake dynamics, electroencephalographic changes and the homeostatic regulation of sleep

Research literature on the effects of photoperiodic manipulations is to my knowledge limited to the effects of photoperiod-induced alterations in a) circadian rhythmicity, gene expression and neuroplasticity of the SCN (Bendova & Sumova, 2006; Buijink et al., 2016; Quiles, de Oliveira, Tonon, & Hidalgo, 2016; VanderLeest et al., 2007), b) brain neurotransmitter profiles (Dulcis, Jamshidi, Leutgeb, & Spitzer, 2013; Green, Jackson, Iwamoto, Tackenberg, & McMahon, 2015), and c) behavioral phenotypes of depression and/or anxiety (Barnes, Smith, & Datta, 2017). There is in fact one study that has examined the effects of altered photoperiod on sleep and EEG; however this study characterized the effects of exposure to shorten circadian photoperiods (21h, 22h and 23h) (Rozov, Zant, Gurevicius, Porkka-Heiskanen, & Panula, 2016). The second part of this thesis is thus the first study to extensively examine how sleep-wake dynamics, electroencephalographic changes, and the homeostatic regulation of sleep are affected by exposure to a prolonged photoperiod.

Additionally, the study is the first of its kind to characterize the differential long-term effects of white vs. blue-enriched light, and to characterize the effects of returning back to a regular light-dark cycle following exposure to prolonged photoperiod.

4.2.1. Exposure to prolonged photoperiod alters sleep-wake dynamics and EEG correlates of arousal

Rats exposed to seven days of prolonged photoperiod in broad spectrum white light spent more time asleep (more total sleep, more SWS), showed stronger sleep consolidation (more SWS and REM sleep bouts) and spent less time awake. In contrast, prolonged blue-enriched light exposure did not exert any changes in time spent in sleep or wakefulness. However, a suppressing effect on beta activity in quiet wakefulness (QW) (a neurophysiological marker of sleep drive) was evident. Thus, prolonged white light exposure induced more sleep (and concomitantly less wakefulness) and increased measures of sleep consolidation, whereas prolonged blue-enriched light exposure had an arousing effect on the brain, indicated by – not only an inhibition – but a *suppression* of beta activity below baseline values.

The findings of sleep-promotion in white light and arousal-promotion in blue-enriched light are in line with recent studies in mice aiming at disentangling the differential effects of light of various spectral intensities. Light is not exclusively sleep-promoting in rodents, as believed previously, rather the behavioral outcome depends on the relative contribution of wavelengths in the electromagnetic spectrum. In mice, green wavelengths have been shown to induce sleep whereas blue wavelengths have been shown to delay sleep induction and increase stress levels. Furthermore, green light was associated with an activation of the VLPO whereas blue light was associated with activation of the SCN and the adrenal glands (Pilorz et al., 2016). Despite the differential responses to green and blue light, both set of responses are

likely mediated by ipRGC signaling. Pilorz and colleagues have put forward the hypothesis that responses to green and blue light are gated through subtypes of ipRGCs projecting to different neural structures implicated in sleep and arousal. Specifically, they postulate that the non-M1 ipRGCs (may it be the M2-M5 or yet-to-be discovered subtypes) are activated by green light and project to sleep-active neurons in the VLPO where they promote sleep. In contrast, M1 ipRGCs are activated by blue light and send projections to the SCN and adrenal glands in where signals of activation and arousal are transmitted throughout the central nervous system. In the following paragraphs I will discuss my findings on sleep-wake dynamics and electrophysiological changes mainly in relation to the hypotheses postulated by Pilorz and colleagues, with an emphasis on the role of sleep-active neurons in the VLPO, and the role of major neural structures involved in the regulation of arousal and alertness. In describing the role of sleep-active VLPO neurons I will briefly touch upon aspects of homeostatic sleep regulation. However these aspects will be further elaborated on in the next section where I aim to discuss photoperiodic effects on the rise and decline of process S in the two-process model of sleep regulation.

In the VLPO, sleep-active neurons of galaninergic and/or GABAergic nature play a role in sleep induction and sleep maintenance by responding to signals of sleep pressure generated by "somnogens" accumulated during wakefulness (such as adenosine and serotonin), and by inhibiting neural structures promoting wakefulness and arousal. The sleep-active neurons are found preferentially in the core of the VLPO (Szymusiak, Alam, Steininger, & McGinty, 1998) and can be separated in two clusters (Gallopin et al., 2005). The first cluster of neurons (type 1) has been shown to be inhibited by serotonergic signaling whereas the second cluster (type 2) has been shown to be excited by adenosine (homeostatic signals) through postsynaptic activation of the adenosine A_{2A} receptor ($A_{2A}R$). Hence, type 1 neurons are likely involved in consolidating sleep throughout the subjective night, in contrast

to type 2 neurons of which are more likely to play a role in the early processes of sleep induction (Gallopin et al., 2005). As previously mentioned, sleep-active neurons of the VLPO are proposed to promote sleep by receiving information from non-M1 ipRGCs maximally activated by light of green wavelengths. From spectrophotometric measurements in the two different light conditions utilized in the rat model of prolonged photoperiod, we know that the spectrum of the white light condition is in large part made up of green wavelengths, in addition to a substantial contribution from red wavelengths (see Figure X). The findings of increased sleep time and reduced time in wakefulness in rats during prolonged photoperiod of white light is thus in line with the proposed model put forward by Pilorz and colleagues. It should be noted that Pilorz exposed mice to light of monochromatic wavelengths, and thus one would expect less clear effects when the light source is of polychromatic nature, as was the case in the rat model of prolonged photoperiod. Also, studies aiming at quantifying light-induced neural activation usually employ c-Fos as a marker (increased c-Fos is indicative of depolarization of neurons in a given area). There is a possibility that a given level of c-Fos in the VLPO during sleep might simply reflect the subsequent state of sleep or wakefulness of the animal rather than providing an indicator of activation caused by light *per se* (Fisk et al., 2018).

Photic information from ipRGCs is relayed to a range of neural structures involved in regulating wakefulness and arousal, included but not limited to the ventral tegmental area (promoting wakefulness through dopaminergic signaling), the lateral hypothalamus (promoting wakefulness through the signaling of orexins), the adrenal glands (producing stress hormones) and the locus coeruleus (promoting alertness through the actions of norepinephrine). Prior to the findings of Pilorz and colleagues it has been shown that a) broadband spectrum white light activates the adrenal glands through projections from the SCN, b) this activation leads to increased levels of plasma and brain corticosterone, and c)

there exists a dose-response relationship between irradiance (intensity of light energy) and the increase in corticosterone (Ishida et al., 2005). Furthermore, the irradiance threshold for light-induced secretion of corticosterone from the adrenal gland has been shown to be higher during the subjective day compared to the subjective night (Kiessling, Sollars, & Pickard, 2014). Pilorz and colleagues showed that blue light activates the adrenal gland and increases corticosterone levels to a greater extent than do light of other wavelengths. Given these results and the observations of an irradiance dose-dependent response in the adrenal gland, it is reasonable to expect a larger activation/alerting response to blue-enriched light compared to white light (due to higher frequency of "blue" wavelengths and thus also higher irradiance). Findings from exposure to 20:4 LD in blue-enriched light is indeed in accordance with previous studies on the effects of blue (-enriched) light on brain and physiology. Even though the rodent model of prolonged photoperiod does not include corticosterone data or data on blue-enriched light-induced neural activation, my findings are in agreement with the hypotheses and points towards an alerting effect of blue-enriched light in the nocturnal rat, indicated by the suppression of beta activity in QW. Contrary to the hypothesis, rats in blue-enriched light did not spend more time asleep neither did they spend less time in wakefulness. The fact that these rats did not spend less time awake despite an extension of "the window of sleep" is further supportive of the alerting effect of blue-enriched light on the central nervous system. Due to the wavelength spectrum of blue-enriched light (that is, the presence of all wavelengths) I would have expected an increase in total sleep time, possibly resulting from the ability of green wavelengths to activate the sleep-active neurons of the VLPO via non-M1 ipRGCs. Given the experimental design I can only speculate about the relative activation of ipRGC subtypes resulting from prolonged blue-enriched light exposure. Nevertheless, my findings illustrate the importance of the relative contribution of different wavelengths to the overall behavioral and/or physiological response of the organism.

Not only is the alerting effect of blue-enriched light gated through effects on the SCN and the adrenal glands but also through projections from ipRGCs to the noradrenergic system of the brainstem. The locus coeruleus system enhances wakefulness, alertness and arousal through dense excitatory projections to the majority of the cortex, basal forebrain, thalamus, dorsal raphe and pedunculo pontine and laterodorsal tegmental nucleus, and some inhibitory projections to GABAergic and/or galaninergic sleep-active neurons in the VLPO (Samuels & Szabadi, 2008). Thus, blue-enriched light might induce arousal and alertness through three major pathways; namely an excitatory route from M1 ipRGCs to the SCN and further on to the adrenal glands, another excitatory route from M1 ipRGCs to the locus coeruleus, and one inhibitory route from locus coeruleus to neurons of the VLPO. To complicate matters further, it has been shown that increased activity in SCN neurons contribute to an inhibition of sleep-active neurons of the VLPO through the actions of norepinephrine (Saint-Mleux et al., 2007). Thus, the alerting effect of blue-enriched light most likely originates from the combined influences of two main processes: 1) an activation of the SCN, adrenals, and locus coeruleus, and 2) an overall inhibition of the VLPO.

4.2.2. Exposure to prolonged photoperiod exerts little effect on the homeostatic regulation of sleep

According to the two-process model of sleep regulation, sleep is regulated by two processes: a circadian process (process C) and a homeostatic process (process S) (Borbély, 1982). Process C is the circadian rhythm being entrained to the ambient light-dark (LD) cycle by ipRGCs transmitting information in the retinohypothalamic tract (RHT). Process S reflects the need for sleep and is represented by a sleep drive that accumulates with time spent awake and dissipates in the course of sleep. EEG SWA in the range of 0.5-4 Hz is considered the neurophysiological marker of sleep drive. In the VLPO, one of the two identified main

clusters of neurons is thought to respond to signals of homeostatic sleep pressure through postsynaptic activation of $A_{2A}R$. The notion of the existence of neurons responding to homeostatic signals of sleep pressure is supported by findings in mice genetically modified to lack the gene coding for the adenosine A_{1A} receptor ($A_{1A}R$). Compared to wild type mice and following sleep deprivation, $A_{1A}R$ deficient mice slept as long as wild type mice, however, they showed an attenuated SWA rebound (Bjorness, Kelly, Gao, Poffenberger, & Greene, 2009). Furthermore, observations indicate that the discharge rate of type 2 neurons mirrors the dynamic alterations in homeostatic sleep pressure. As sleep pressure increases, type 2 neurons increase their firing rate; both during the sleep deprivation period and during subsequent recovery sleep (Alam, Kumar, McGinty, Alam, & Szymusiak, 2013).

Our rat model of prolonged photoperiod in 20:4 LD represents a condition in where process S have been manipulated by extending the hours of light within the 24h. The time of light onset (ZT0) is not changed but the "window of sleep" during inactive (light) phase is extended (from 12 to 20h), and the active (dark) phase is compressed to 4h. In this study, the rise of process S was quantified by a mathematical modeling approach whereas the decline of process S was quantified both by the use of a mathematical model and by examining the decline of EEG SWA in SWS, at ZT0, ZT2, ZT5, and ZT11. Even though rats in both light conditions showed a normal decline in homeostatic sleep pressure from ZT0 to ZT2, exposure to a prolonged photoperiod did not alter this decline as compared to baseline. Observations from mice housed in symmetrical short photoperiods (10.5:10.5 LD, 11:11 LD, 11.5:11.5 LD) indicate an opposite influence on the decline in sleep pressure. In short symmetrical photoperiods, mice showed an increase in SWA during SWS, indicating elevated sleep pressure (Rozov et al., 2016). However, although these photoperiods indeed were "short" they were also symmetrical and hence, comparing these results to the results of my "asymmetrical" 20:4 photoperiod is somewhat problematic. If the photoperiodic manipulation in Rozov et al.

had been of such a nature that the active phase was prolonged and the inactive phase was compressed, the relevance to findings from an "opposite" pattern (20:4 LD) would be clearer.

The only photoperiod-induced effect of 20:4 LD on the decline in SWA was seen in rats exposed to prolonged photoperiod of white light. These rats had an increased level of SWA in ZT11 (the last hour of inactive phase). No such increase was observed in animals exposed to prolonged photoperiod in blue-enriched light. The observation of elevated SWA in ZT11 after prolonged white light exposure contradicts the hypothesis on reduced sleep pressure as a consequence of extending the "window of sleep" and compressing the active phase of the animal. By compressing the active phase, one would expect an attenuated accumulation of "somnogens" (such as adenosine) during wakefulness (reduced build-up of sleep pressure), and hence the type 2 neurons of the VLPO would be insufficiently activated and exhibit reduced firing rate during SWS, and the level of SWA during SWS would be reduced (due to attenuated build-up of sleep pressure (EEG SWA) during wakefulness). The finding of elevated SWA in ZT11 in rats exposed to prolonged photoperiod white light is not in accordance with the aforementioned mechanisms of homeostatic sleep regulation, neither is the finding compatible with observations indicating that the concentration of adenosine A_1 receptors is reduced in the prefrontal cortex of rats exposed to 16:8 LD (Chennaoui et al., 2017).

In rats exposed to prolonged photoperiod in blue-enriched light I expected an inhibition of SWA during SWS. Descriptively, such an inhibition was indeed true for the blue-enriched light condition, some of which might be a possible explanation for the lack of influence of 20:4 LD blue-enriched light on the homeostatic decline in sleep pressure. Thus, additive to the aforementioned mechanisms of reduced accumulation of "somnogens" during wakefulness – subsequent decreased firing rate of VLPO type 2 neurons – and reduced SWA in SWS during 20:4 LD, there might be a mechanism of action involving VLPO type 2

neurons responding not only to homeostatic signals generated from the expenditure of energy during hours spent awake but also responding to energy from light itself.

4.2.3. Sleep-wake dynamics and EEG are altered in the recovery from a prolonged photoperiod

Upon return to standard 12:12 LD conditions, rats exposed to prolonged photoperiod displayed changes in sleep-wake dynamics and EEG. Following prolonged white light exposure, effects on sleep-wake dynamics were of minor nature and the effects persisted for 3 recovery days only. Throughout recovery day 1 to 3, rats had more REM sleep bouts and the duration of wakefulness bouts was shorter. Additionally, they spent less time in active wakefulness (AW). Descriptively, the increases in SWA during SWS observed at day 7 of prolonged photoperiod persisted throughout the entire recovery period (although small effect size). Thus, results indicate that sleep-wake dynamics are easily recovered in 12:12 LD, however the small white-light induced modulation in SWA during SWS seem to last over days, possibly involving an adaption in the sleep-active neurons of the VLPO.

Following prolonged blue-enriched light exposure, a rebound in sleep dynamics were evident for up to 5 recovery days. Rats from the blue-enriched light condition slept longer and they had more SWS and REM sleep bouts. Moreover, the effects on wake-dynamics were delayed until recovery day 3, and some of these effects persisted to day 7 of recovery. From recovery day 3 to 7, rats spent less time awake, they spent less time in AW, and the duration of wakefulness bouts was shortened. The observed alerting effect of blue-enriched light on SWA and beta activity during exposure to prolonged photoperiod persisted throughout the entire recovery period in 12:12 LD, indicating a strong adaption of the neural systems receiving information from the blue light-sensitive photoreceptors of the retina.

Thus, the changes in sleep and wakefulness induced by prolonged white light exposure were normalized after 3 days of recovery in standard 12:12 LD. In contrast, being exposed to 20:4 LD in blue-enriched light exerts a strong effect on the sleep-wake regulatory systems, as evidenced by a rebound in sleep-wake dynamics for up to 7 recovery days and a prominent alerting effect on the brain. Moreover, recovery data following 20:4 LD blue-enriched light supports the proposed inhibitory effect of blue-enriched light on neural systems involved in sleep induction and sleep maintenance. A blue-enriched light-induced inhibition of the sleep-active neurons in the VLPO during exposure to 20:4 is consistent with a rebound effect in sleep parameters during the recovery period.

4.2.4. Homeostatic regulation of sleep is affected in the recovery from a prolonged photoperiod

The typical decline in sleep pressure from ZT0 to ZT2, as observed in baseline, was not evident throughout the first 5 days of recovery following prolonged photoperiod in white light. At recovery day 7, the normal decline in SWA from ZT0 to ZT2 was recovered. In addition to a non-existent decline in sleep pressure throughout most of the recovery period, rats exposed to prolonged white light displayed alterations in the levels of SWA throughout inactive phase for up to 5 recovery days. The observation of elevated SWA in ZT11 during exposure to prolonged photoperiod was also present at the first day of recovery. Again, this finding is not in accordance with the aforementioned neurophysiological- and biological mechanisms underlying homeostatic sleep regulation. However, at recovery day 3 and 5, rats from the white light condition had lower levels of SWA in ZT0 (the first hour of lights on). Although this effect was hypothesized to be present during exposure to prolonged photoperiod (attenuated build-up of sleep pressure in active phase, and hence reduced levels

of SWA at sleep onset), the presence of such an effect in recovery period might indicate that the sleep homeostat takes some time to adjust to an altered light-dark environment.

Following exposure to prolonged photoperiod in blue-enriched light, rats displayed a normal reduction in homeostatic sleep pressure from ZT0 to ZT2 throughout most of the recovery period. However, the levels of SWA were altered throughout inactive phase, and the effects were present throughout the entire recovery period. Upon returning back to 12:12 LD following prolonged blue-enriched light, the level of SWA was increased in ZT5 and in ZT11 for the first 3 recovery days. This might be a rebound effect of the blue-enriched light-induced suppression of SWA during prolonged photoperiod. Throughout the rest of the recovery period, prolonged exposure to blue-enriched light induced a reduction in the levels of SWA in ZT0 (first hour of lights on). The reduction was still present at day 7 of recovery. Again, this effect was hypothesized to be present during prolonged photoperiod, and the effect (that is, attenuated build-up of sleep pressure in active phase, and subsequently reduced levels of SWA at sleep onset) was expected to be stronger for blue-enriched light compared to white light. The presence of a reduction in SWA in ZT0 in the recovery period following blue-enriched light exposure likely involves several mechanisms working in concert. However, one plausible mechanism is an adaptation of the arousal systems during prolonged photoperiod, such that the combined influence of blue-enriched light-induced inhibition of the VLPO and excitation of the SCN, adrenal glands and the locus coeruleus overrides any other mechanisms trying to re-balance the sleep homeostat. Irrespective of the possible mechanisms underlying these effects, my results clearly indicate that the alerting effect of blue-enriched light exposure persists for at least 7 days following the termination of prolonged photoperiod.

In discussing findings on homeostatic sleep regulation in rats exposed to and recovering from prolonged photoperiod, it should be mentioned that a limitation already resides in the two-process model itself. Although the homeostatic and circadian regulation of

sleep is similar across humans and rodents, the polyphasic nature of rodent sleep is not accounted for by the two-process model of sleep regulation. Despite suggestions to include the polyphasic nature of rodent sleep in model I am aware of only one actual attempt in doing so (Rempe et al., 2018).

4.2.5. Implications of findings

Although the field of research on light, sleep and brain activity is quite young, the explosion of studies in the past five years all points towards strong negative effects of exposure to blue wavelengths at inappropriate times of day. This exposure largely comes from the use of LED screens, particularly in the evening and at night. By suppressing SWA during SWS, blue-enriched light exerts a negative influence on the quality of sleep. The results of this study supports other findings of an alerting effect of blue-enriched light exposure, and speaks of the importance of reducing blue-enriched light during the evening and subjective night.

The findings of this study have implications for the general population aiming at healthier light exposure, clinical groups at risk of blue-enriched light-induced alterations in psychiatric stat, and people working night shifts. The alerting effect of blue-enriched light might be particularly important to avoid in those individuals at risk of entering bipolar mania, as indicated by results from an RCT in this patient group showing the effectiveness of blocking out blue wavelengths by the use of blue-blocking glasses (Henriksen et al., 2016).

Light may also be beneficial, at the wrong time of day. The alerting effect of blue-enriched light might be advantageous in reducing sleepiness in people working night shifts. Studies in humans and rodents indicate that prolonged periods of wakefulness induce deficits in alertness, mood, memory and cognitive performance (Banks & Dinges, 2007; Havekes, Meerlo, & Abel, 2015). In an established rodent model of shift work (Grønli, Janne et al.,

2017; Marti et al., 2016), Grønli and colleagues have shown that simulated night shift work is associated with degradations in waking behavior, indicated by the presence of increased slow-wave energy (the accumulation of SWA across time) in quiet wakefulness during night shifts. Findings from the rat model of prolonged photoperiod indicates that blue-enriched light suppresses beta activity in quiet wakefulness and hence, exposure to blue-enriched light during the night shift might counteract some of the negative effects on sleepiness and cognitive performance in night shift workers.

4.2.5. Strength and limitation

Although the study has several strong points, it is still associated with some limitations that should be noted. The use of blue-enriched polychromatic light instead of monochromatic blue light represents both a limitation and strength of the present study. By using blue-enriched polychromatic light, the interpretation of findings is less clear due to the differential activation of the retinal photoreceptors to all wavelengths. However compared to monochromatic blue light, blue-enriched light is a much more natural condition for a rodent (living outside being exposed to dusk, dawn and blue-enriched light from the sun) and hence, the rat model of prolonged photoperiod exhibits higher ecological validity than had it done if the light exposure was of monochromatic nature. The fact that I could have been able to interpret the effects of prolonged photoperiod in a more robust manner had I used a recently developed tool box for the quantification of physiological responses of the rodent eye to light energy. In this tool box one simply plots the values obtained from a spectrophotometric measurement and the output shows the differential activation of photopigments inherent in the photoreceptors.

Due to the fact that the overall sample size was somewhat limited, subtle differences in the effect of prolonged photoperiod on sleep would go undetected because of statistical power limitations.

Additionally I have only characterized the long-term effects of prolonged photoperiod (at exposure day 7) and in the recovery thereof. I do have scored EEG/EMG for the entire week of exposure to prolonged photoperiod, and thus, a limitation of the present experiment is the lack of a characterization throughout experimental condition. Several studies indicate that the sleep-wake systems (and the brain plasticity) adapt to light over time, and thus reporting results from exposure day 1 to 7 will give a picture of the short-term dynamics of change. Similarly, the recovery data reported here is only a fraction of the available data analysed.

Last, a limitation is inherent in the two-process model itself, of which I discuss my findings, due to the fact that the polyphasic nature of sleep in a nocturnal rodent is not accounted for in the model equations of the rise and decline of process S. In order to clean out some of the "noise" in EEG SWA resulting from the lack of polyphasic modelling, I could have utilized the approach as described in different laboratories; Paul Franken at Univeristé de Lausanne, Switzerland and Robert Greene at University of Texas, US. Both Dr. Franken and Dr.Greene use only the longest SWS bouts into account (those of 5 min duration or longer) and hence the reduction in SWA during SWS becomes more salient.

4.2.6. Future directions

The present rat model of prolonged photoperiod has characterized the effects of sleep-wake dynamics, electrophysiological changes and the homeostatic regulation at day 7 of light exposure only. Thus, future research should aim at characterizing the dynamics in these effects throughout the entire 7 days of prolonged photoperiod. Moreover, a wide range of data from the same rat model of 20:4 LD has been collected; including data on circadian

rhythmicity, neuroplasticity markers in the brain, and behavioral changes. The present rat model has characterized the effects of 7 recovery days, however 7-14 more recovery days exist in the data set and future attempts should be made in characterizing the effects on sleep, wakefulness, EEG and homeostatic sleep regulation, both in standard 12:12 LD conditions and in DD (continuous darkness) conditions in order to examine whether some of the effects are circadian-driven and of endogenous nature. Furthermore, future research should aim at characterizing for how long there is a suppression of beta activity in QW following exposure to prolonged photoperiod in blue-enriched light, and also whether a possible change in neuroplasticity markers may mirror the changes observed in the EEG resulting from prolonged photoperiod. Previous studies in rats indicate that exposure to prolonged photoperiod may induce behavioral changes associated with phenotypes of depression and/or anxiety. Future research should hence establish whether exposure to prolonged photoperiod induces behavioral changes, and whether blue-enrich light exerts a different effect than white light.

5. Conclusion

Results from the validation of a semi-automatic sleep scoring algorithm show that the algorithm was in good agreement with a manual gold standard. When comparing scoring performance of the algorithm in four experimental groups of rats exposed to different photoperiodic manipulations, the inter-rater agreement between algorithm and manual soring was strong and the inter-rater reliability was almost perfect, for short photoperiod white light. For short photoperiod blue-enriched light, long photoperiod white light and long photoperiod blue-enriched light, inter-rater reliability and inter-rater agreement was substantial.

Seven days of exposure to prolonged photoperiod in white light induced changes in sleep-wake dynamics and sleep consolidation, and minor changes in the homeostatic

regulation of sleep. Exposure to prolonged blue-enriched light did not exert any influence on sleep-wake dynamics, sleep consolidation and homeostatic sleep regulation; instead, blue-enriched light induced a suppression of beta activity during quiet wakefulness, indicative of an alerting effect.

Following prolonged white light exposure, effects on sleep-wake dynamics were of minor nature and the effects persisted for 3 recovery days only. Following prolonged blue-enriched light exposure, a rebound in sleep dynamics were evident for up to 5 recovery days. The homeostatic decline in sleep pressure was altered for up to 5 days following prolonged photoperiod white light, and for the entire recovery period following blue-enriched light condition. The suppressing effect of blue-enriched light on beta activity in quiet wakefulness persisted throughout the entire recovery period. Thus, results points towards an alerting effect of blue-enriched light and that the effect persists for at least one week in normal light conditions.

References

Alam, Kumar, McGinty, Alam, & Szymusiak. (2013). Neuronal activity in the preoptic hypothalamus during sleep deprivation and recovery sleep. *Journal of neurophysiology, 111*(2), 287-299.

Altimus, Güler, Villa, McNeill, Legates, & Hattar. (2008). Rods-cones and melanopsin detect light and dark to modulate sleep independent of image formation. *Proceedings of the National Academy of Sciences, 105*(50), 19998-20003.

Aschoff. (1965). Circadian rhythms in man. *Science, 148*(3676), 1427-1432.

Bailes, & Lucas. (2013). Human melanopsin forms a pigment maximally sensitive to blue light (λmax≈ 479 nm) supporting activation of Gq/11 and Gi/o signalling cascades. *Proc. R. Soc. B, 280*(1759), 20122987.

Banks, & Dinges. (2007). Behavioral and physiological consequences of sleep restriction. *Journal of clinical sleep medicine: JCSM: official publication of the American Academy of Sleep Medicine, 3*(5), 519.

Barnes, Smith, & Datta. (2017). Beyond emotional and spatial processes: cognitive dysfunction in a depressive phenotype produced by long photoperiod exposure. *PloS one, 12*(1), e0170032.

Bastianini, Berteotti, Gabrielli, Del Vecchio, Amici, Alexandre, . . . Martire. (2014). SCOPRISM: a new algorithm for automatic sleep scoring in mice. *Journal of neuroscience methods, 235*, 277-284.

Bauer, Glenn, Alda, Andreassen, Angelopoulos, Ardau, . . . Bellivier. (2015). Influence of light exposure during early life on the age of onset of bipolar disorder. *Journal of psychiatric research, 64*, 1-8.

Bauer, Glenn, Alda, Andreassen, Ardau, Bellivier, . . . Del Zompo. (2012). Impact of sunlight on the age of onset of bipolar disorder. *Bipolar disorders, 14*(6), 654-663.

Bendova, & Sumova. (2006). Photoperiodic regulation of PER1 and PER2 protein expression in rat peripheral tissues. *Physiological research, 55*(6), 623.

Berger. (1930). Uber das elektrenkephalogramm des menschen. II. *J Psychol Neurol (Leipzig), 40*, 160-179.

Berry, Brooks, Gamaldo, Harding, Marcus, & Vaughn. (2012). The AASM manual for the scoring of sleep and associated events. *Rules, Terminology and Technical Specifications, Darien, Illinois, American Academy of Sleep Medicine*.

Berson, Dunn, & Takao. (2002). Phototransduction by retinal ganglion cells that set the circadian clock. *Science, 295*(5557), 1070-1073.

Bjorness, Kelly, Gao, Poffenberger, & Greene. (2009). Control and function of the homeostatic sleep response by adenosine A1 receptors. *Journal of Neuroscience, 29*(5), 1267-1276.

Borbély. (1982). A two process model of sleep regulation. *Hum neurobiol, 1*(3), 195-204.

Borbély, Baumann, Brandeis, Strauch, & Lehmann. (1981). Sleep deprivation: effect on sleep stages and EEG power density in man. *Electroencephalography and clinical neurophysiology, 51*(5), 483-493.

Borbely, & Neuhaus. (1979). Sleep-deprivation: effects on sleep and EEG in the rat. *Journal of comparative physiology, 133*(1), 71-87.

Borbély, Tobler, & Hanagasioglu. (1984). Effect of sleep deprivation on sleep and EEG power spectra in the rat. *Behavioural brain research, 14*(3), 171-182.

Buijink, Almog, Wit, Roethler, Engberink, Meijer, . . . Michel. (2016). Evidence for weakened intercellular coupling in the mammalian circadian clock under long photoperiod. *PloS one, 11*(12), e0168954.

Chang, Aeschbach, Duffy, & Czeisler. (2015). Evening use of light-emitting eReaders negatively affects sleep, circadian timing, and next-morning alertness. *Proceedings of the National Academy of Sciences, 112*(4), 1232-1237.

Chang, Santhi, St Hilaire, Gronfier, Bradstreet, Duffy, . . . Czeisler. (2012). Human responses to bright light of different durations. *The Journal of physiology, 590*(13), 3103-3112.

Chellappa, Steiner, Oelhafen, Lang, Götz, Krebs, & Cajochen. (2013). Acute exposure to evening blue-enriched light impacts on human sleep. *Journal of sleep research, 22*(5), 573-580.

Chennaoui, Arnal, Dorey, Sauvet, Ciret, Gallopin, . . . Gomez-Merino. (2017). Changes of Cerebral and/or Peripheral Adenosine A1 Receptor and IGF-I Concentrations under Extended Sleep Duration in Rats. *International journal of molecular sciences, 18*(11), 2439.

Cohen. (1960). A coefficient of agreement for nominal scale. *Educ Psychol Meas, 20*, 37-46.

Cohen. (1992). A power primer. *Psychol Bull, 112*(1), 155-159.

Czeisler, Shanahan, Klerman, Martens, Brotman, Emens, . . . Rizzo. (1995). Suppression of melatonin secretion in some blind patients by exposure to bright light. *New England Journal of Medicine, 332*(1), 6-11.

Dulcis, Jamshidi, Leutgeb, & Spitzer. (2013). Neurotransmitter switching in the adult brain regulates behavior. *Science, 340*(6131), 449-453.

Fisk, Tam, Brown, Vyazovskiy, Bannerman, & Peirson. (2018). Light and Cognition: Roles for Circadian Rhythms, Sleep, and Arousal. *Frontiers in neurology, 9*, 56.

Franken, Tobler, & Borbély. (1995). Varying photoperiod in the laboratory rat: profound effect on 24-h sleep pattern but no effect on sleep homeostasis. *American Journal of Physiology-Regulatory, Integrative and Comparative Physiology, 269*(3), R691-R701.

Freedman, Lucas, Soni, von Schantz, Muñoz, David-Gray, & Foster. (1999). Regulation of mammalian circadian behavior by non-rod, non-cone, ocular photoreceptors. *Science, 284*(5413), 502-504.

Gallopin, Luppi, Cauli, Urade, Rossier, Hayaishi, . . . Fort. (2005). The endogenous somnogen adenosine excites a subset of sleep-promoting neurons via A2A receptors in the ventrolateral preoptic nucleus. *Neuroscience, 134*(4), 1377-1390.

Gilmour, Fang, Guan, & Subramanian. (2010). Manual rat sleep classification in principal component space. *Neuroscience letters, 469*(1), 97-101.

Golombek, & Rosenstein. (2010). Physiology of circadian entrainment. *Physiological reviews, 90*(3), 1063-1102.

Gooley, Lu, Fischer, & Saper. (2003). A broad role for melanopsin in nonvisual photoreception. *Journal of Neuroscience, 23*(18), 7093-7106.

Green, Jackson, Iwamoto, Tackenberg, & McMahon. (2015). Photoperiod programs dorsal raphe serotonergic neurons and affective behaviors. *Current Biology, 25*(10), 1389-1394.

Gringras, Middleton, Skene, & Revell. (2015). Bigger, brighter, bluer-better? current light-emitting devices–adverse sleep properties and preventative strategies. *Frontiers in public health, 3*, 233.

Grønli, Byrkjedal, Bjorvatn, Nødtvedt, Hamre, & Pallesen. (2016). Reading from an iPad or from a book in bed: the impact on human sleep. A randomized controlled crossover trial. *Sleep medicine, 21*, 86-92.

Grønli, Meerlo, Pedersen, Pallesen, Skrede, Marti, . . . Rempe. (2017). A rodent model of night-shift work induces short-term and enduring sleep and electroencephalographic disturbances. *Journal of biological rhythms, 32*(1), 48-63.

Grønli, Rempe, Clegern, Schmidt, & Wisor. (2016). Beta EEG reflects sensory processing in active wakefulness and homeostatic sleep drive in quiet wakefulness. *Journal of sleep research, 25*(3), 257-268.

Grønli, & Ursin. (2009). Basic sleep mechanisms. *Tidsskrift for den Norske laegeforening: tidsskrift for praktisk medicin, ny raekke, 129*(17), 1758-1761.

Hannibal. (2002). Neurotransmitters of the retino-hypothalamic tract. *Cell and tissue research, 309*(1), 73-88.

Hattar, Kumar, Park, Tong, Tung, Yau, & Berson. (2006). Central projections of melanopsin-expressing retinal ganglion cells in the mouse. *Journal of Comparative Neurology, 497*(3), 326-349.

Hattar, Liao, Takao, Berson, & Yau. (2002). Melanopsin-containing retinal ganglion cells: architecture, projections, and intrinsic photosensitivity. *Science, 295*(5557), 1065-1070.

Havekes, Meerlo, & Abel. (2015). Animal studies on the role of sleep in memory: from behavioral performance to molecular mechanisms. In *Sleep, Neuronal Plasticity and Brain Function* (pp. 183-206): Springer.

Henriksen, Skrede, Fasmer, Schoeyen, Leskauskaite, Bjørke-Bertheussen, . . . Lund. (2016). Blue-blocking glasses as additive treatment for mania: a randomized placebo-controlled trial. *Bipolar disorders, 18*(3), 221-232.

Ishida, Mutoh, Ueyama, Bando, Masubuchi, Nakahara, . . . Okamura. (2005). Light activates the adrenal gland: timing of gene expression and glucocorticoid release. *Cell metabolism, 2*(5), 297-307.

Kayumov, Casper, Hawa, Perelman, Chung, Sokalsky, & Shapiro. (2005). Blocking low-wavelength light prevents nocturnal melatonin suppression with no adverse effect on

performance during simulated shift work. *The Journal of Clinical Endocrinology & Metabolism, 90*(5), 2755-2761.

Keenan, & Hirshkowitz. (2017). Sleep Stage Scoring. In *Principles and Practice of Sleep Medicine (Sixth Edition)* (pp. 1567-1575. e1563): Elsevier.

Kiessling, Sollars, & Pickard. (2014). Light stimulates the mouse adrenal through a retinohypothalamic pathway independent of an effect on the clock in the suprachiasmatic nucleus. *PloS one, 9*(3), e92959.

Landis, & Koch. (1977). An application of hierarchical kappa-type statistics in the assessment of majority agreement among multiple observers. *Biometrics*(Jun;33(2):), 363-374.

Libourel, Corneyllie, Luppi, Chouvet, & Gervasoni. (2015). Unsupervised online classifier in sleep scoring for sleep deprivation studies. *Sleep, 38*(5), 815-828.

Lockley, Evans, Scheer, Brainard, Czeisler, & Aeschbach. (2006). Short-wavelength sensitivity for the direct effects of light on alertness, vigilance, and the waking electroencephalogram in humans. *Sleep, 29*(2), 161-168.

Lucas, Freedman, Muñoz, Garcia-Fernández, & Foster. (1999). Regulation of the mammalian pineal by non-rod, non-cone, ocular photoreceptors. *Science, 284*(5413), 505-507.

Lupi, Oster, Thompson, & Foster. (2008). The acute light-induction of sleep is mediated by OPN4-based photoreception. *Nature neuroscience, 11*(9), 1068.

Marti, Meerlo, Grønli, van Hasselt, Mrdalj, Pallesen, . . . Skrede. (2016). Shift in food intake and changes in metabolic regulation and gene expression during simulated night-shift work: a rat model. *Nutrients, 8*(11), 712.

McGinty, & Szymusiak. (2017). Neural control of sleep in mammals. In *Principles and Practice of Sleep Medicine (Sixth Edition)* (pp. 62-77. e65): Elsevier.

Moore, & Lenn. (1972). A retinohypothalamic projection in the rat. *Journal of Comparative Neurology, 146*(1), 1-14.

Moscardo, & Rostello. (2010). An integrated system for video and telemetric electroencephalographic recording to measure behavioural and physiological parameters. *Journal of pharmacological and toxicological methods, 62*(1), 64-71.

Muindi, Zeitzer, Colas, & Heller. (2013). The acute effects of light on murine sleep during the dark phase: importance of melanopsin for maintenance of light-induced sleep. *European Journal of Neuroscience, 37*(11), 1727-1736.

Panda, Nayak, Campo, Walker, Hogenesch, & Jegla. (2005). Illumination of the melanopsin signaling pathway. *Science, 307*(5709), 600-604.

Pelayo, & Dement. (2017). History of sleep physiology and medicine. In *Principles and Practice of Sleep Medicine (Sixth Edition)* (pp. 3-14. e14): Elsevier.

Pilorz, Tam, Hughes, Pothecary, Jagannath, Hankins, . . . Nolan. (2016). Melanopsin regulates both sleep-promoting and arousal-promoting responses to light. *PLoS biology, 14*(6), e1002482.

Provencio, Rodriguez, Jiang, Hayes, Moreira, & Rollag. (2000). A novel human opsin in the inner retina. *Journal of Neuroscience, 20*(2), 600-605.

Provencio, Wong, Lederman, Argamaso, & Foster. (1994). Visual and circadian responses to light in aged retinally degenerate mice. *Vision research, 34*(14), 1799-1806.

Quiles, de Oliveira, Tonon, & Hidalgo. (2016). Biological adaptability under seasonal variation of light/dark cycles. *Chronobiology international, 33*(8), 964-971.

Rahman, Flynn-Evans, Aeschbach, Brainard, Czeisler, & Lockley. (2014). Diurnal spectral sensitivity of the acute alerting effects of light. *Sleep, 37*(2), 271-281.

Reis, Hebenstreit, Gabsteiger, von Tscharner, & Lochmann. (2014). Methodological aspects of EEG and body dynamics measurements during motion. *Frontiers in human neuroscience, 8*, 156.

Rempe, Clegern, & Wisor. (2015). An automated sleep-state classification algorithm for quantifying sleep timing and sleep-dependent dynamics of electroencephalographic and cerebral metabolic parameters. *Nature and science of sleep, 7*, 85.

Rempe, Grønli, Pedersen, Mrdalj, Marti, Meerlo, & Wisor. (2018). Mathematical Modeling of Sleep State Dynamics in a Rodent Model of Shift Work. *Neurobiology of Sleep and Circadian Rhythms*.

Roenneberg, & Foster. (1997). Twilight times: light and the circadian system. *Photochemistry and photobiology, 66*(5), 549-561.

Rozov, Zant, Gurevicius, Porkka-Heiskanen, & Panula. (2016). Altered Electroencephalographic Activity Associated with Changes in the Sleep-Wakefulness Cycle of C57BL/6J Mice in Response to a Photoperiod Shortening. *Frontiers in behavioral neuroscience, 10*, 168.

Rytkönen, Zitting, & Porkka-Heiskanen. (2011). Automated sleep scoring in rats and mice using the naive Bayes classifier. *Journal of neuroscience methods, 202*(1), 60-64.

Rångtell, Ekstrand, Rapp, Lagermalm, Liethof, Búcaro, . . . Benedict. (2016). Two hours of evening reading on a self-luminous tablet vs. reading a physical book does not alter sleep after daytime bright light exposure. *Sleep medicine, 23*, 111-118.

Sahin, Wood, Plitnick, & Figueiro. (2014). Daytime light exposure: Effects on biomarkers, measures of alertness, and performance. *Behavioural brain research, 274*, 176-185.

Saint-Mleux, Bayer, Eggermann, Jones, Mühlethaler, & Serafin. (2007). Suprachiasmatic modulation of noradrenaline release in the ventrolateral preoptic nucleus. *Journal of Neuroscience, 27*(24), 6412-6416.

Samuels, & Szabadi. (2008). Functional neuroanatomy of the noradrenergic locus coeruleus: its roles in the regulation of arousal and autonomic function part I: principles of functional organisation. *Current neuropharmacology, 6*(3), 235-253.

Sasseville, Paquet, Sévigny, & Hébert. (2006). Blue blocker glasses impede the capacity of bright light to suppress melatonin production. *Journal of pineal research, 41*(1), 73-78.

Scammell, Arrigoni, & Lipton. (2017). Neural circuitry of wakefulness and sleep. *Neuron, 93*(4), 747-765.

Schmidt, Chen, & Hattar. (2011). Intrinsically photosensitive retinal ganglion cells: many subtypes, diverse functions. *Trends in neurosciences, 34*(11), 572-580.

Stockman, & Sharpe. (2000). The spectral sensitivities of the middle-and long-wavelength-sensitive cones derived from measurements in observers of known genotype. *Vision research, 40*(13), 1711-1737.

Szymusiak, Alam, Steininger, & McGinty. (1998). Sleep–waking discharge patterns of ventrolateral preoptic/anterior hypothalamic neurons in rats. *Brain research, 803*(1-2), 178-188.

Tobler, Borbely, & Groos. (1983). The effect of sleep deprivation on sleep in rats with suprachiasmatic lesions. *Neuroscience letters, 42*(1), 49-54.

Tsai, Hannibal, Hagiwara, Colas, Ruppert, Ruby, . . . Bourgin. (2009). Melanopsin as a sleep modulator: circadian gating of the direct effects of light on sleep and altered sleep homeostasis in Opn4−/− mice. *PLoS biology, 7*(6), e1000125.

Tsao, Coltrin, Crawford, & Simmons. (2010). Solid-state lighting: an integrated human factors, technology, and economic perspective. *Proceedings of the IEEE, 98*(7), 1162-1179.

van der Lely, Frey, Garbazza, Wirz-Justice, Jenni, Steiner, . . . Schmidt. (2015). Blue blocker glasses as a countermeasure for alerting effects of evening light-emitting diode screen exposure in male teenagers. *Journal of Adolescent Health, 56*(1), 113-119.

VanderLeest, Houben, Michel, Deboer, Albus, Vansteensel, . . . Meijer. (2007). Seasonal encoding by the circadian pacemaker of the SCN. *Current Biology, 17*(5), 468-473.

Vandewalle, Balteau, Phillips, Degueldre, Moreau, Sterpenich, . . . Dang-Vu. (2006). Daytime light exposure dynamically enhances brain responses. *Current Biology, 16*(16), 1616-1621.

Vandewalle, Schmidt, Albouy, Sterpenich, Darsaud, Rauchs, . . . Luxen. (2007). Brain responses to violet, blue, and green monochromatic light exposures in humans: prominent role of blue light and the brainstem. *PloS one, 2*(11), e1247.

Vyazovskiy, & Tobler. (2005). Theta activity in the waking EEG is a marker of sleep propensity in the rat. *Brain research, 1050*(1-2), 64-71.

Wright Jr, McHill, Birks, Griffin, Rusterholz, & Chinoy. (2013). Entrainment of the human circadian clock to the natural light-dark cycle. *Current Biology, 23*(16), 1554-1558.

6. Appendix

6.1. Appendix A – Baseline Analyses

Table I

Results from Baseline analyses on Sleep, Wakefulness, EEG and Process S Modelling

	Effect of day		
	F	df	p
TST	2.44	1,10	NS
Time in SWS	1.86	1,10	NS
SWS bout duration	0.59	1,10	NS
Number of SWS bouts	0.01	1,10	NS
Time in REM sleep	2.35	1,10	NS
REM sleep bout duration	0.68	1,10	NS
Number of REM sleep bouts	0.1	1,10	NS
Time in wakefulness	2.32	1,10	NS
Time in AW	2.36	1,10	NS
Time in QW	2.31	1,10	NS
Wake bout duration	0.53	1,10	NS
Number of wake bouts	0.24	1,10	NS
SWA in SWS	0.75	1,10	NS
Beta activity in AW	0.36	1,10	NS
Beta activity in QW	0.14	1,10	NS
Ti	1.78	1,10	NS
UA	0.29	1,10	NS
Td	1.97	1,10	NS
LA	0.01	1,10	NS

One-way ANOVA for main effects of light on sleep, wakefulness, EEG and output parameters from mathematical modelling of process S in baseline. F and p values of main effects are indicated for all parameters studied. NS denotes non-significance.

Abbreviations: TST total sleep time; SWS slow-wave sleep; REM rapid eye movement; AW active wake; QW quiet wake; SWA slow-wave activity; Ti rising time constant; UA upper asymptote; Td declining time constant; LA lower asymptote.

Table II

Results from Baseline analyses on Homeostatic reduction in Sleep Pressure

		Decline in SWA during SWS
Effect of ZT	F	**17.27**
	df	**4,40**
	p	**<0.001**
Effect of light	F	1.53
	df	1,10
	p	NS
Interaction effect (light x ZT)	F	0.12
	df	4,40
	p	NS

Repeated measures ANOVA for main effects of ZT and light on the homeostatic reduction in sleep pressure, assessed by the decline in SWA during SWS, in baseline. F and p values of main effects are indicated. NS denotes non-significance.

Abbreviations: ZT zeitgeber; SWA slow-wave activity; SWS slow-wave sleep.

6.2. Appendix B – Analyses from Prolonged Photoperiod

Table III

Experimental effects on Sleep, Wakefulness, EEG and Process S Modelling in Prolonged Photoperiod

	Effect of day			Effect of light			Interaction effect (day x light)		
	F	df	p	F	df	p	F	df	p
TST	**13.72**	**1,10**	**0.004**	1.36	1,10	NS	2.33	1,10	NS
SWS	**9.56**	**1,10**	**0.011**	1.01	1,10	NS	1.25	1,10	NS
SWS bout duration	2.76	1,10	NS	0.32	1,10	NS	1.24	1,10	NS
Number of SWS bouts	**8.11**	**1,10**	**0.017**	0.04	1,10	Ns	0.09	1,10	NS
REMS	1.48	1,10	NS	2.54	1,10	NS	0.72	1,10	NS
REMS bout duration	4.38	1,10	NS	1.53	1,10	NS	1.52	1,10	NS
Number of REMS bouts	**7.46**	**1,10**	**0.021**	0.13	1,10	NS	2.94	1,10	NS
Total wakefulness	**14.28**	**1,10**	**0.004**	1.42	1,10	NS	1.51	1,10	NS
AW	**5.24**	**1,10**	**0.045**	1.49	1,10	NS	0.26	1,10	NS
QW	0.76	1,10	NS	1.16	1,10	NS	0.14	1,10	NS
Wake bout duration	**12.87**	**1,10**	**0.005**	0.47	1,10	NS	0.44	1,10	NS
Number of wake bouts	4.65	1,10	NS	0.18	1,10	NS	0.10	1,10	NS
SWA in SWS	0.17	1,10	NS	0.72	1,10	NS	0.50	1,10	NS
Beta activity in AW	1.00	1,10	NS	0.50	1,10	NS	0.02	1,10	NS
Beta activity in QW	**5.41**	**1,10**	**0.042**	0.02	1,10	NS	**9.57**	**1,10**	**0.011**
Ti	0.47	1,10	NS	0.01	1,10	NS	3.82	1,10	NS
UA	4.66	1,10	NS	0.12	1,10	NS	2.65	1,10	NS
Td	0.76	1,10	NS	1.02	1,10	NS	3.42	1,10	NS
LA	2.22	1,10	NS	0.00	1,10	NS	0.18	1,10	NS

Results of repeated measures ANOVA for main effects of day and light and interaction effects between day and light on sleep, wakefulness, EEG and output parameters from mathematical modelling of process S. F and p values of main and interaction effects are indicated for all parameters studied. NS denotes non-significance.

Abbrevations: TST total sleep time; SWS slow-wave sleep; REMS rapid eye movement sleep; AW active wake; QW quiet wake; SWA slow-wave activity; Ti rising time constant; UA upper asymptote; Td declining time constant; LA lower asymptote.

Table IIII

Effects of day, light and zeitgeber on the Homeostatic reduction of Sleep Pressure in Prolonged Photoperiod

		Decline in SWA during SWS
Effect of day	F	1.23
	df	1,9
	p	NS
Effect of light	F	0.01
	df	1,9
	p	NS
Effect of ZT	F	**24.37**
	df	**3,27**
	p	**<0.001**
Interaction effect (day x light)	F	0.92
	df	1,9
	p	NS
Interaction effect (day x ZT)	F	**3.94**
	df	**3,27**
	p	**0.019**
Interaction effect (light x ZT)	F	1.28
	df	3,37
	p	NS
Interaction effect (day x light x ZT)	F	0.16
	df	3,27
	p	NS

Results from repeated measures ANOVA for main and interaction effects of day, light and ZT on the homeostatic reduction in sleep pressure, assessed by the decline of SWA during SWS. F and p values of main and interaction effects are indicated. NS denotes non-significance. Abbreviations: ZT zeitgeber; SWA slow-wave activity; SWS slow-wave sleep.

6.3. Appendix C – Analyses from the Recovery Period following Prolonged Photoperiod

Table V

Effects on Sleep, Wakefulness, EEG and Process S Modelling in Recovery from prolonged photoperiod

	Effect of day			Effect of light			Interaction effect (day x light)		
	F	df	p	F	df	p	F	df	p
TST	**2.84**	**4,40**	**0.037**	2.28	1,10	NS	1.88	4,40	NS
SWS	1.78	4,40	NS	1.74	1,10	NS	1.70	4,40	NS
SWS bout duration	1.31	4,40	NS	0.17	1,10	NS	0.92	4,40	NS
Number of SWS bouts	**3.32**	**4,40**	**0.019**	0.1	1,10	NS	0.33	4,40	NS
REMS	**2.63**	**4,40**	**0.049**	3.48	1,10	NS	0.33	4,40	NS
REMS bout duration	1.35	4,40	NS	0.81	1,10	NS	0.29	4,40	NS
Number of REMS bouts	**6.09**	**4,40**	**<0.001**	0.00	1,10	NS	0.66	4,40	NS
Total wakefulness	**2.78**	**4,40**	**0.040**	2.22	1,10	NS	1.71	4,40	NS
AW	**7.55**	**4,40**	**<0.001**	1.94	1,10	NS	0.85	4,40	NS
QW	2.13	4,40	NS	2.49	1,10	NS	1.61	4,40	NS
Wake bout duration	**4.59**	**4,40**	**0.004**	0.23	1,10	NS	1.65	4,40	NS
Number of wake bouts	2.28	4,40	NS	0.14	1,10	NS	0.43	4,40	NS
SWA in SWS	0.53	4,40	NS	0.77	1,10	NS	0.20	4,40	NS
Beta activity in AW	1.74	4,40	NS	0.03	1,10	NS	1.62	4,40	NS
Beta activity in QW	2.17	4,40	NS	0.00	1,10	NS	**6.13**	**4,40**	**<0.001**
Ti	1.11	4,36	NS	1.02	1,9	NS	0.80	4,36	NS
UA	0.47	4,36	NS	0.06	1,9	NS	1.05	4,36	NS
Td	0.79	4,36	NS	0.18	1,9	NS	1.35	4,36	NS
LA	1.53	4,36	NS	0.05	1,9	NS	0.92	4,36	NS

Results of repeated measures ANOVA for main effects of days and light and interaction effects between days and light on sleep, wakefulness, EEG, and output parameters from mathematical modelling of process S. F and p values of main and interaction effects are indicated for all parameters studied. NS denotes non-significance.

Abbrevations: TST total sleep time; SWS slow-wave sleep; REMS rapid eye movement sleep; AW active wake; QW quiet wake; SWA slow-wave activity; Ti rising time constant; UA upper asymptote; Td declining time constant; LA lower asymptote.

Table VI

Effects of days, light and zeitgeber on the Homeostatic reduction of Sleep Pressure in Recovery from prolonged photoperiod

		Decline in SWA during SWS
Effect of days	F	**6.62**
	df	**4,36**
	p	**<0.001**
Effect of light	F	1.66
	df	1,9
	p	NS
Effect of ZT	F	**32.04**
	df	**3,27**
	p	**<0.001**
Interaction effect (days x light)	F	0.75
	df	4,36
	p	NS
Interaction effect (days x ZT)	F	**2.30**
	df	**12,108**
	p	**0.012**
Interaction effect (light x ZT)	F	1.73
	df	3,27
	p	NS
Interaction effect (days x light x ZT)	F	0.79
	df	12,108
	p	NS

Results from repeated measures ANOVA for main and interaction effects of days, light and ZT on the decline of SWA in SWS. F and p values of main and interaction effects are indicated. NS denotes non-significance.
Abbreviations: ZT zeitgeber; SWA slow-wave activity; SWS slow-wave sleep.

Table VII

Light group comparisons of % change in SWA during SWS in the recovery period

	t	df	p
R1	-0.95	10	NS
R3	-0.80	10	NS
R5	-0.84	10	NS
R7	-0.61	10	NS

Results of independent-samples t-test for between-group comparisons (white vs. blue-enriched light) on % change in SWA from baseline, at recovery day 1 (R1), 3 (R3), 5 (R5) and (R7). T and p values of group effect are indicated. NS denotes non-significance. Abbreviations: SWA slow-wave activity; SWS slow-wave sleep.